

Complexes of Ag(I), Hg(I) and Hg(II) with multidentate pyrazolyl-pyridine ligands: from mononuclear complexes to coordination polymers *via* helicates, a mesocate, a cage and a catenate

Stephen P. Argent,^a Harry Adams,^a Thomas Riis-Johannessen,^b John C. Jeffery,^b Lindsay P. Harding,^c William Clegg,^{d,e} Ross W. Harrington^d and Michael D. Ward^{*a}

Received 30th May 2006, Accepted 15th August 2006

First published as an Advance Article on the web 7th September 2006

DOI: 10.1039/b607541j

The coordination chemistry of a series of di- and tri-nucleating ligands with Ag(I), Hg(I) and Hg(II) has been investigated. Most of the ligands contain two or three *N,N'*-bidentate chelating pyrazolyl-pyridine units pendant from a central aromatic spacer; one contains three binding sites (2 + 3 + 2-dentate) in a linear sequence. A series of thirteen complexes has been structurally characterised displaying a wide range of structural types. Bis-bidentate bridging ligands react with Ag(I) to give complexes in which Ag(I) is four-coordinate from two bidentate donors, but the complexes can take the form of one-dimensional coordination polymers, or dinuclear complexes (mesocate or helicate). A tris-bidentate triangular ligand forms a complicated two-dimensional coordination network with Ag(I) in which Ag...Ag contacts, as well as metal–ligand coordination bonds, play a significant role. Three dinuclear Hg(I) complexes were isolated which contain an {Hg₂}²⁺ metal–metal bonded core bound to a single bis-bidentate ligand which can span both metal ions. Also characterised were a series of Hg(II) complexes comprising a simple mononuclear four-coordinate Hg(II) complex, a tetrahedral Hg^{II}₄ cage which incorporates a counter-ion in its central cavity, a trinuclear double helicate, and a trinuclear catenated structure in which two long ligands have spontaneously formed interlocked metallomacrocyclic rings thanks to cyclometallation of two of the Hg(II) centres.

Introduction

It is a well understood principle in metallosupramolecular chemistry that the structures of complexes based on the combination of multidentate bridging ligands with labile metal ions is a compromise between the geometric properties of the ligands (number and arrangement of binding sites; flexibility) and the stereoelectronic properties of the metal ion.^{1–5} In many cases the careful exploitation of these principles has allowed rational design of elaborate polynuclear assemblies such as helicates,² grids³ and cages⁴ from relatively simple components. In other cases, the complexity of the metal complex assemblies—whilst conforming to the basic principles outlined—is nonetheless remarkable given the simplicity of the component parts.^{1,5}

We have described recently a series of dinucleating and trinucleating bridging ligands in which two or three bidentate, chelating, pyrazolyl-pyridine units are connected *via* methylene spacers to

aromatic spacers.⁵ On reaction with first-row transition metal dications, having a preference for pseudo-octahedral coordination geometry, these have afforded a range of polyhedral coordination cages varying in complexity from tetrahedra containing four metal ions and six bridging ligands to tetra-capped-truncated tetrahedra containing 16 metal ions and 24 bridging ligands. In all cases, the preference of the metal ion for six-coordinate geometry has provided an essential piece of geometric information which plays an important role in the assembly of the cage complexes. The ligands relevant to this paper are shown in Scheme 1. The '2 + 3 + 2'-dentate ligand L²³² is constituted slightly differently, with a linear sequence of three binding sites which are either bidentate (pyrazolyl-pyridine) or terdentate [2,6-bis(pyrazol-3-yl)pyridine]; this ligand was used to prepared trinuclear double helicates with a range of metal ions, including a mixed-metal [FeAg₂(L²³²)₂]⁴⁺ containing two four-coordinate Ag(I) ions at the terminal sites and a six-coordinate Fe(II) ion at the central site.^{5j}

In this paper we describe the coordination chemistry of this series of ligands with Ag(I), Hg(I) and Hg(II), which have quite different stereo-electronic properties and may be expected to generate quite different metal/ligand assemblies. In particular the 'soft' nature of Ag(I) and Hg(I) means that they tend to adopt coordination numbers lower than six, and are also subject to strong metal–metal bonding interactions^{6,7} which are absent for first-row transition metal dications.

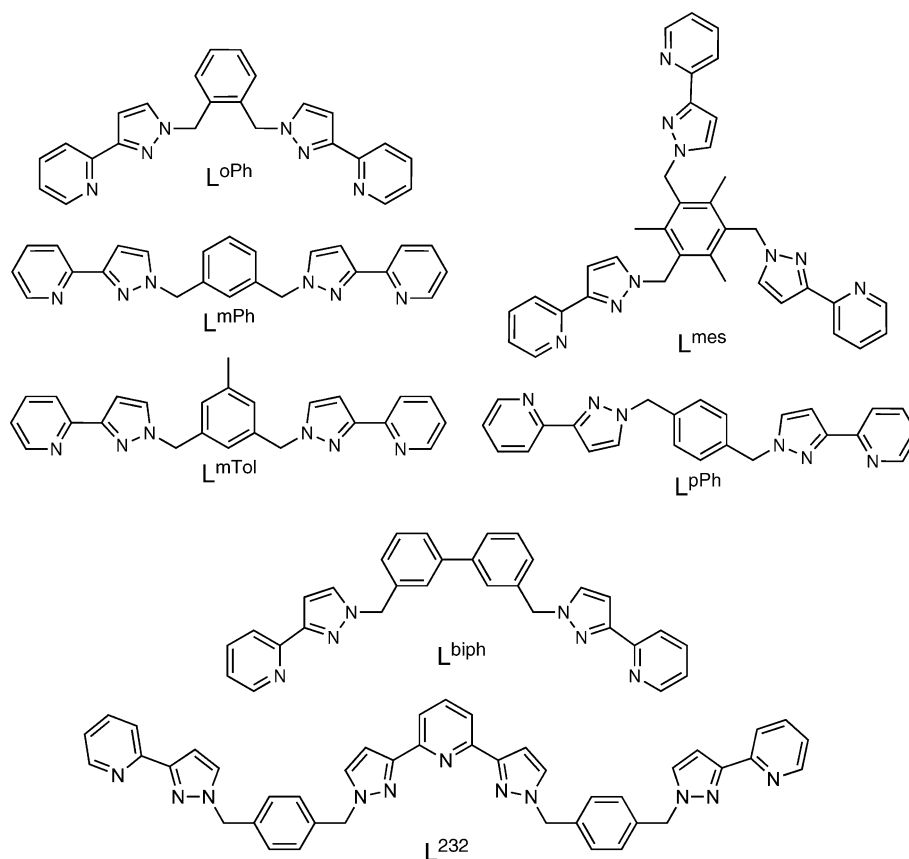
^aDepartment of Chemistry, University of Sheffield, Sheffield, UK S3 7HF. E-mail: m.d.ward@sheffield.ac.uk

^bSchool of Chemistry, University of Bristol, Cantock's Close, Bristol, UK BS8 1TS

^cDepartment of Chemical and Biological Sciences, University of Huddersfield, Huddersfield, UK HD1 3DH

^dSchool of Natural Sciences (Chemistry), University of Newcastle, Newcastle upon Tyne, UK NE1 7RU

^eCCLRC Daresbury Laboratory, Warrington, UK WA4 4AD



Scheme 1

Results and discussion

Ligands

The ligands used for the work in this paper are illustrated in Scheme 1; the majority have been reported before, but L^{mTol} is new. Like the others,⁵ it was prepared by reaction of 3-(2-pyridyl)pyrazole with the appropriate bis(bromomethyl)-substituted organic spacer, in this case 1-methyl-3,5-bis(bromomethyl)benzene, in the presence of aqueous NaOH under phase-transfer conditions. Satisfactory characterisation data were obtained (see Experimental).

Complexes of Ag(I) with L^{mPh} , L^{mTol} and L^{pPh} . The reaction of L^{mPh} with $[\text{Ag}(\text{MeCN})_4][\text{BF}_4]$ in a 1 : 1 ratio in acetonitrile gave a colourless solution. Slow diffusion of diisopropyl ether

into this solution gave colourless crystals whose elemental analysis indicates a 1 : 1 stoichiometry $\text{Ag}(L^{\text{mPh}})(\text{BF}_4)$. The crystal structure (Fig. 1, Table 1) shows the solid state arrangement to be an infinite one-dimensional helical coordination polymer with the formula $[\text{Ag}(L^{\text{mPh}})(\text{BF}_4)(^i\text{Pr}_2\text{O})]_{\infty}$. The asymmetric unit of the crystals contains one formula unit. Each Ag(I) ion is four-coordinate,

Table 1 Selected bond lengths (Å) and angles (°) for $[\text{Ag}(L^{\text{mPh}})\text{BF}_4](^i\text{Pr}_2\text{O})_{\infty}$

Ag(1)–N(41)	2.228(3)	N(41)–Ag(1)–N(11)	153.60(11)
Ag(1)–N(11)	2.252(3)	N(41)–Ag(1)–N(21)	125.03(11)
Ag(1)–N(21)	2.385(3)	N(11)–Ag(1)–N(21)	73.28(11)
Ag(1)–N(51)	2.425(4)	N(41)–Ag(1)–N(51)	71.48(11)
		N(11)–Ag(1)–N(51)	122.75(12)
		N(21)–Ag(1)–N(51)	111.80(11)

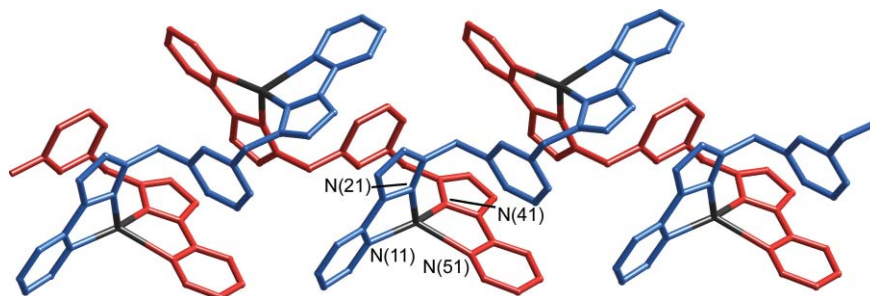


Fig. 1 The one-dimensional helical chain structure of $[\text{Ag}(L^{\text{mPh}})(\text{BF}_4)(^i\text{Pr}_2\text{O})]_{\infty}$ (anions and solvent molecules not shown). Ligands are shown with alternating red and blue colours for clarity, but are all crystallographically equivalent. The Ag(I) ions are in black.

chelated by pyrazolyl-pyridine units from two separate ligands. Each ligand bridges between two metal ions and is related to the next by a two-fold rotation and translation giving the helix a periodicity of two Ag(I) ions. The Ag(I) ions follow a zig-zag path with an Ag–Ag–Ag internal angle of 88.9° and Ag–Ag separations of 8.06 Å. Equal numbers of each enantiomer of helix are packed together as parallel chains.

The Ag(I) ion is coordinated in a distorted four-coordinate environment with two shorter bonds to the pyridyl donors (average 2.24 Å) and two longer bonds to the pyrazolyl donors (average 2.41 Å) with a twist angle between the Ag(NN) planes of 88.6°. Within the chains, interligand π – π stacking interactions (separation 3.2–3.5 Å) are observed between phenyl spacers of one ligand and the pyrazolyl-pyridine unit of an adjacent ligand. Stacking interactions like these are a common feature of one-dimensional coordination polymers with aromatic ligands.⁸ The arrangement of the helical polymer is such that only one of the pyrazolyl-pyridyl arms is involved in these stacking interactions. There are no stacking interactions between the ligands of adjacent parallel chains. BF₄[–] counterions and (disordered) diisopropyl ether molecules are located in channels running parallel to the polymeric chains.

In CD₃CN solution the ¹H NMR spectrum of [Ag(L^{mPh})(BF₄)]_∞ shows that the ligand has characteristic chemical shifts for metal coordination at the pyrazolyl-pyridine donors, and has two-fold symmetry. The ES mass spectrum shows strong peaks at *m/z* 499.1 {Ag(L^{mPh})⁺} and 1087.2 {Ag₂(L^{mPh})₂(BF₄)⁺} and a series of much smaller peaks for higher oligomers of the formula {Ag_{*n*}(L^{mPh})_{*n*}(BF₄)_{*n-2*}}²⁺ (*n* = 6–10). This suggests that the dinuclear entity {Ag₂(L^{mPh})₂}²⁺ exists to a significant extent in solution, consistent with the observation by ¹H NMR of symmetrically coordinated ligand. The only obvious reason why this should dominate in solution is if it is in fact a discrete dinuclear complex with two ligand bridging two metal ions (*e.g.* a double helicate), rather just a fragment from the coordination polymer breaking up. The polymer observed in the solid state may therefore be a kinetic crystallisation product nucleated by the small concentration of higher oligomers in solution observed in the mass spectrum.⁹ We note that other examples of helical coordination polymers with Ag(I) have been described recently.^{8,10}

Examination of the crystal structure of [Ag(L^{mPh})(BF₄)(^{*i*}Pr₂O)]_∞ suggested that a substituent attached to the vacant *meta* position of the central phenylene unit would hinder formation of this coordination polymer by generating an unfavourable steric interaction with the next ligand in the sequence. Accordingly we prepared the new ligand L^{mTol}, reaction of which with [Ag(MeCN)₄][X] (X = BF₄ or ClO₄) in a 1 : 1 ratio in acetonitrile gave a colourless solution. Slow diffusion of diisopropyl ether into this solution gave colourless crystals in each case whose elemental analysis indicates a 1 : 1 stoichiometry of Ag(L^{mTol})X. The crystal structures showed an essentially identical structure in each case, but the data for the structure of the fluoroborate salt were poor so we describe here only the structure of the perchlorate salt. X-Ray analysis shows the solid state structure of the complex to be a dinuclear ‘mesocate’ with formula [Ag₂(L^{mTol})₂][ClO₄]₂, in which both ligands span both metal ions but in an achiral arrangement such that the complex is not a helicate (Fig. 2, Table 2). Mesocates frequently occur when ligand geometry and metal stereochemical preferences disfavour the twist which imparts chirality into related

Table 2 Selected bond lengths (Å) and angles (°) for [Ag₂(L^{mTol})₂][ClO₄]₂

Ag(1)–N(41A)	2.423(2)	N(41A)–Ag(1)–N(11)	110.75(8)
Ag(1)–N(11)	2.310(2)	N(41A)–Ag(1)–N(51A)	72.10(8)
Ag(1)–N(51A)	2.248(2)	N(11)–Ag(1)–N(51A)	154.79(8)
Ag(1)–N(21)	2.311(2)	N(41A)–Ag(1)–N(21)	130.80(8)
		N(11)–Ag(1)–N(21)	72.45(8)
		N(51A)–Ag(1)–N(21)	125.82(8)

Symmetry operations used to generate equivalent atoms: A, $-x, 2 - y, -z$

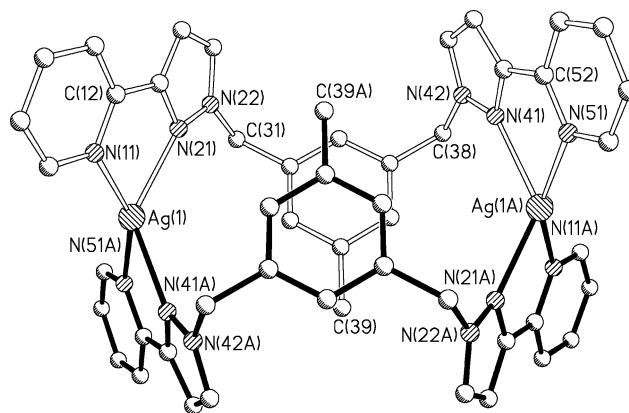


Fig. 2 The dinuclear cation of [Ag₂(L^{mTol})₂][ClO₄]₂. Ligands are shown with different colours for clarity but are crystallographically equivalent.

helicates.¹¹ The complex cation lies on an inversion centre such that the asymmetric unit contains one complete ligand, one Ag(I) ion and a perchlorate counterion. Each Ag(I) ion is four-coordinate, chelated by pyrazolyl-pyridine units from two separate ligands. The donor units of each ligand approach both Ag(I) ions from the same direction without the twist observed in ligands which form helicates. The separation between the Ag(I) ions is 8.23 Å, marginally larger than that observed in the polymer [Ag(L^{mPh})(BF₄)(^{*i*}Pr₂O)]_∞.

The Ag(I) ions are in a distorted tetrahedral environment with Ag–N bond lengths in the range 2.28–2.42 Å and a twist angle between the Ag(NN) planes of 59.8°. A π – π stacking interaction is observed between the two phenyl spacer rings (separation 3.70 Å). The rings are offset across the inversion centre such that each methyl group [C(39)] is located above the centre of the other ring. Within the unit cell, individual mesocate cations are stacked in columns with the phenyl spacers of adjacent cations facing each other. Each cation is rotated by 120° with respect to the one above it in order to allow intermolecular π – π stacking interactions between the phenyl spacer rings (separation 3.4–3.7 Å). These stacking interactions, combined with the intramolecular stacking previously described, give rise to infinite arrays of stacked phenyl rings along the axis of the columns. Further stacking interactions are observed between the pyrazolyl-pyridine rings of cations in adjacent columns (separation 3.3–3.4 Å). Counterions are located in channels between the columns.

In CD₃CN solution the ¹H NMR spectrum of [Ag₂(L^{mTol})₂][BF₄]₂ in acetonitrile is consistent with a two-fold symmetric ligand coordinated to metal ions at the pyrazolyl-pyridine binding sites, as also observed for [Ag(L^{mPh})(BF₄)]_∞. An upfield shift of 0.85 ppm for the protons of the methyl group

(1.42 ppm) compared to the free ligand (2.27 ppm) is observed due to the shielding effect of the adjacent phenyl ring. The ES mass spectrum is also similar to that of $[\text{Ag}(\text{L}^{\text{mPh}})(\text{BF}_4)]_\infty$, with strong peaks at m/z 513.1 $\{\text{Ag}(\text{L}^{\text{mTol}})\}^+$ and 1115.2 $\{\text{Ag}_2(\text{L}^{\text{mTol}})_2(\text{BF}_4)_2\}^+$ and a series of much smaller peaks for higher oligomers of the formula $\{\text{Ag}_n(\text{L}^{\text{mTol}})_n(\text{BF}_4)_{n-2}\}^{2+}$ ($n = 6-10$). These observations indicate similar solution behaviour to that of $[\text{Ag}(\text{L}^{\text{mPh}})(\text{BF}_4)]_\infty$, with the predominant species being a dimer $\{\text{Ag}_2(\text{L}^{\text{mTol}})_2\}^{2+}$ with two-fold symmetry. The upfield shift of the methyl protons arising from a ring current effect association with π -stacking of the tolyl rings is also consistent with the retention of the solid state structure in solution. Again, minor traces of higher oligomers are still detected in the mass spectrum, though in this case it seems the methyl groups inhibit the crystallisation of the polymeric species and only the dimer crystallises.

The ligand L^{pPh} features a more divergent *para*-phenylene spacer with a greater separation between the donor groups. The reaction of L^{pPh} with $[\text{Ag}(\text{MeCN})_4](\text{BF}_4)$ in a 1 : 1 ratio in acetonitrile gave a colourless solution. Slow diffusion of diisopropyl ether into this solution gave colourless crystals whose elemental analysis indicates a 1 : 1 stoichiometry of $\text{Ag}(\text{L}^{\text{pPh}})(\text{BF}_4)$. The crystal structure shows this complex to be a dinuclear double helicate $[\text{Ag}_2(\text{L}^{\text{pPh}})_2][\text{BF}_4]_2$ with two ligands spanning both Ag(I) ions, which are separated by 8.40 Å (Fig. 2, Table 3). Each Ag(I) ion is four coordinate, bound to an *N,N*-chelating unit from each of the two ligands; the geometry is highly distorted from tetrahedral. Equal numbers of opposite enantiomers of helicate are present in the unit cell.

Although the Ag(I) ions are four-coordinate, two shorter contacts (2.26–2.30 Å) from the pyridyl donors describe a nearly linear geometry (N–Ag–N angles of 164.3 and 167.9°). The two longer contacts (2.41–2.47 Å) from the pyrazolyl donors are pinched closer together by the conformation of the helicate (N–Ag–N angles of 118.6 and 115.6°). The twist angles between the Ag(NN) planes of 68.0 and 69.1° underline the large distortion from ideal tetrahedral geometry around the metal ions. The two ligands are in different environments, distinguished by the orientations of the phenyl rings of the spacer units. In the case of ligand A (white in Fig. 3) the phenyl ring is orientated approximately parallel to, and sandwiched between, the two pyrazolyl-pyridine units of ligand B (black in Fig. 3) generating a three-component π -stack with separations between components of 3.4–3.5 Å. In contrast, the phenyl ring of ligand B is rotated such that it is perpendicular to the pyrazolyl-pyridine units of ligand A, resulting in edge-to-face stacking in which the H atoms H(83) and H(86) of the central phenyl ring of ligand B are directed towards the pyridyl rings of

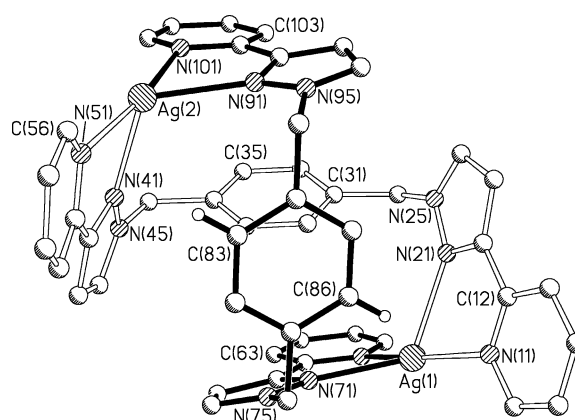


Fig. 3 The dinuclear cation of $[\text{Ag}_2(\text{L}^{\text{pPh}})_2][\text{BF}_4]_2$. Ligands are shown with different colours for clarity.

ligand A. The closest contacts are 2.84 Å [H(83)⋯C(52)] and 2.71 Å [H(86)⋯N(11)]. Thus, the solid-state structure of this double helicate shows a mixture of face-to-face and edge-to-face interactions of aromatic rings between the two ligands which in the solid are in quite different environments.

In solution the ES mass spectrum indicates retention of a dimer structure with peaks at 1085.2 $\{\text{Ag}_2(\text{L}^{\text{pPh}})_2(\text{BF}_4)_2\}^{1+}$ and 500.1 $\{\text{Ag}_2(\text{L}^{\text{pPh}})_2\}^{2+}$. The number and location of the peaks in the ^1H NMR spectrum in acetonitrile is consistent with a two-fold symmetric ligand coordinated to Ag(I) at the pyrazolyl-pyridine groups. The two-fold ligand symmetry indicates that the two distinct ligand environments observed in the crystal structure are exchanging with each other on the NMR timescale, most likely by rotation of the phenyl rings around the axis between the CH_2 groups. The signal for the four protons of the phenyl ring is shifted up-field to 6.02 ppm (from 7.22 ppm in the free ligand), consistent with retention of the aromatic stacking observed for this ring in the crystal structure. The spectrum remained unchanged at -40°C , notably with no splitting of the signal for the CH_2 protons into different environments, indicating that the energetic barrier to this fluxional process is low.

Complexes of Ag(I) with L^{biph} : a pair of one-dimensional coordination polymers. Ligand L^{biph} has a larger biphenyl spacer unit which positions the donor groups even further apart. It has previously been used for the synthesis of large M_4L_6 tetrahedral cages with six-coordinate Co(II); the large size of the cages allowed exchange of internal and external counter-ions which could be monitored by NMR spectroscopy.^{5c} Reaction of L^{biph} with $[\text{Ag}(\text{MeCN})_4](\text{BF}_4)$ in a 1 : 1 ratio in either nitromethane or dmf gave a colourless solution from which in each case colourless crystals could be isolated whose elemental analysis indicates a 1 : 1 stoichiometry of $\text{Ag}(\text{L}^{\text{biph}})(\text{BF}_4)$. Structural analysis revealed in each case one-dimensional coordination polymers with different conformations according to whether or not the uncoordinated solvent molecules could be encapsulated in a channel along the core of the chain.

Crystals of $[\text{Ag}(\text{L}^{\text{biph}})(\text{BF}_4)(\text{MeNO}_2)]_\infty$ diffracted very weakly, resulting in large atomic displacement parameters and standard uncertainties for the resulting structural determination. Despite this, the gross structure is clear and shows that the complex is an infinite one-dimensional helical coordination polymer with

Table 3 Selected bond lengths (Å) and angles (°) for $[\text{Ag}_2(\text{L}^{\text{pPh}})_2][\text{BF}_4]_2$

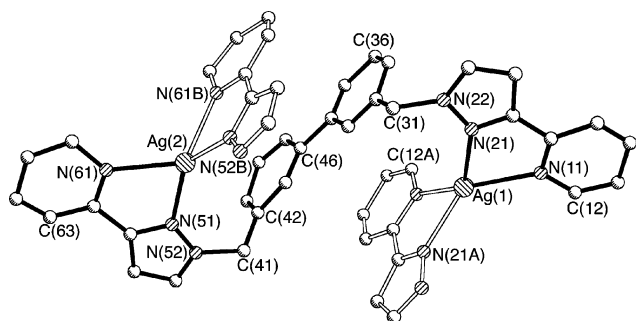
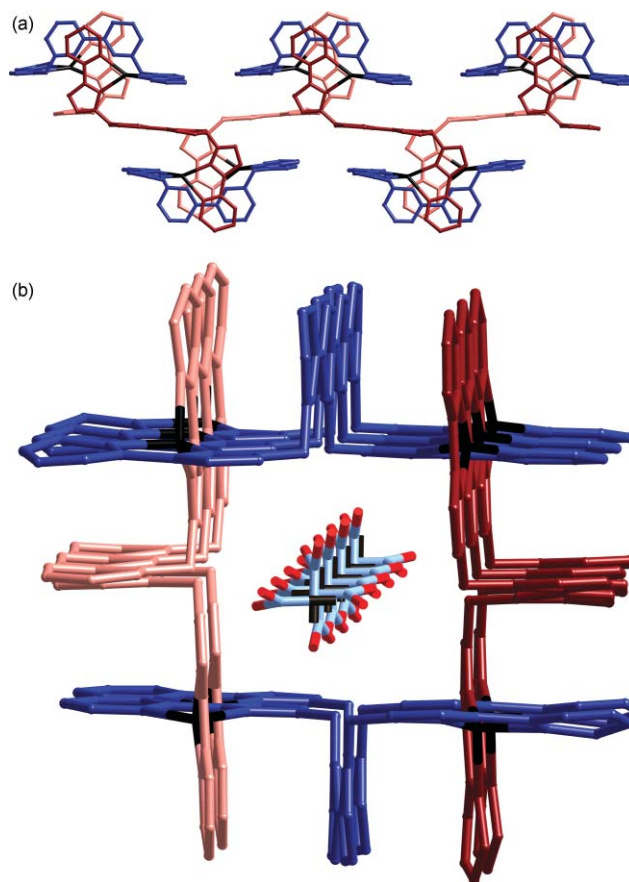
Ag(1)–N(11)	2.264(3)	Ag(2)–N(51)	2.255(3)
Ag(1)–N(61)	2.302(3)	Ag(2)–N(101)	2.278(3)
Ag(1)–N(71)	2.403(3)	Ag(2)–N(91)	2.406(3)
Ag(1)–N(21)	2.472(3)	Ag(2)–N(41)	2.456(3)
N(11)–Ag(1)–N(61)	164.33(11)	N(51)–Ag(2)–N(101)	167.89(11)
N(11)–Ag(1)–N(71)	124.26(10)	N(51)–Ag(2)–N(91)	119.51(10)
N(61)–Ag(1)–N(71)	71.40(10)	N(101)–Ag(2)–N(91)	72.48(10)
N(11)–Ag(1)–N(21)	71.22(10)	N(51)–Ag(2)–N(41)	72.38(10)
N(61)–Ag(1)–N(21)	102.86(9)	N(101)–Ag(2)–N(41)	101.56(10)
N(71)–Ag(1)–N(21)	118.63(11)	N(91)–Ag(2)–N(41)	115.62(10)

Table 4 Selected bond lengths (Å) and angles (°) for $[\text{Ag}(\text{L}^{\text{biph}})(\text{BF}_4)(\text{MeNO}_2)]_\infty$

Ag(1)–N(11)	2.380(14)	Ag(2)–N(51)	2.271(13)
Ag(1)–N(21)	2.327(12)	Ag(2)–N(61)	2.417(19)
N(21)–Ag(1)–N(21A)	126.9(6)	N(51)–Ag(2)–N(51B)	139.3(8)
N(21)–Ag(1)–N(11A)	130.5(4)	N(51)–Ag(2)–N(61B)	133.7(6)
N(21)–Ag(1)–N(11)	71.2(5)	N(51)–Ag(2)–N(61)	71.2(7)
N(11A)–Ag(1)–N(11)	137.1(6)	N(61B)–Ag(2)–N(61)	115.9(12)

Symmetry transformations used to generate equivalent atoms: A: $-x + 9/4, y, -z + 5/4$ B: $-x + 7/4, -y + 3/4, z$

the asymmetric unit containing one formula unit comprising one complete ligand and two half-occupancy metal ions on special positions. Each Ag(I) ion is four-coordinate, bound by *N,N*-chelating units from the pyrazolyl-pyridyl units of two separate ligands; each ligand bridges two Ag(I) ions (Fig. 4 and 5, Table 4). The polymer is generated by a four-fold rotation and translation of the crystallographically unique $\{\text{Ag}(\text{L}^{\text{biph}})\}^+$ units, giving the helix a periodicity of four Ag(I) ions with an alternating sequence of Ag(1) and Ag(2) centres and an $\text{Ag} \cdots \text{Ag}$ separation of 8.52 Å between every adjacent pair of Ag(I) ions. The Ag(I) ions four units apart (directly above each other along the helical axis) are separated by 16.61 Å; this defines the pitch of the helix. Looking down the helical axis the four Ag(I) ions define the corners of a square with the ligands bridging between them. A narrow channel, *ca.* 3 Å across, is enclosed within this square and contains the MeNO₂ solvent molecules (Fig. 5b); in this end-on view the ‘cross-section’ of the chain is approximately 17×17 Å. The two Ag(I) ions are in typical pseudo-tetrahedral coordination environments with Ag–N bond lengths of 2.27–2.42 Å and dihedral angles between the two Ag(NN) planes of 89° at Ag(1) and 74° at Ag(2). Intramolecular aromatic π -stacking interactions occur between every pyridine ring and phenyl spacer ring of its neighbouring ligand (separations ≈ 3.5 Å). The crystal packing shows equal numbers of opposite-handed helices aligned parallel to each other. Inter-chain aromatic stacking interactions occur between the pyridine rings at the corners defined by Ag(1) where opposite-handed chains interpenetrate. The BF₄[−] counterions are located in the cavities at the corners of the spirals between the Ag(I) ions that lie four units (*i.e.* one helical period) apart.

**Fig. 4** Asymmetric unit of $[\text{Ag}(\text{L}^{\text{biph}})(\text{BF}_4)(\text{MeNO}_2)]_\infty$ showing the labelling scheme (H atoms, anions and solvent molecules omitted for clarity). The pyrazolyl-pyridine units with hollow bonds are from adjacent asymmetric units and are included to illustrate the coordination sphere around Ag(1) and Ag(2).**Fig. 5** Two views of the helical chain in the structure of $[\text{Ag}(\text{L}^{\text{biph}})(\text{BF}_4)(\text{MeNO}_2)]_\infty$. (a) A side-on view of a chain; all ligands are crystallographically equivalent but are coloured differently for clarity. (b) A view along a helical chain (looking along the crystallographic *b* axis) showing how MeNO₂ solvent molecules lie in the channel within the helical chain.

The crystals isolated from dmf–diisopropyl ether proved to be $[\text{Ag}(\text{L}^{\text{biph}})(\text{BF}_4)(\text{Pr}_2\text{O})_{0.5}(\text{dmf})_{0.25}]_\infty$ (Fig. 6 and 7, Table 5). The gross structure of this is similar to that of the nitromethane solvate, being a one-dimensional chain with a periodicity of four Ag(I) ions (Fig. 7a), two of which are crystallographically independent. The different metal cations do not alternate, but form the sequence $\{\text{Ag}(1)\text{–Ag}(1)\text{–Ag}(2)\text{–Ag}(2)\}_\infty$ such that there are different $\text{Ag} \cdots \text{Ag}$ separations; these are 9.61 Å $[\text{Ag}(1) \cdots \text{Ag}(1)]$;

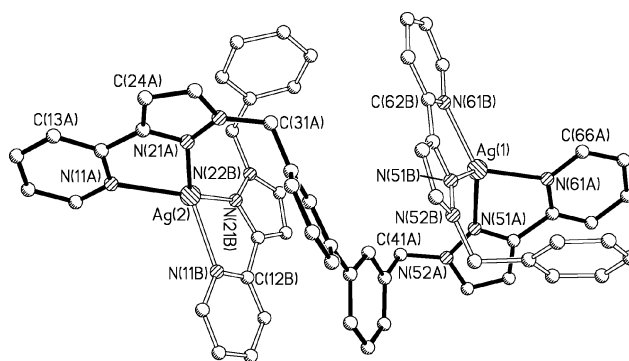
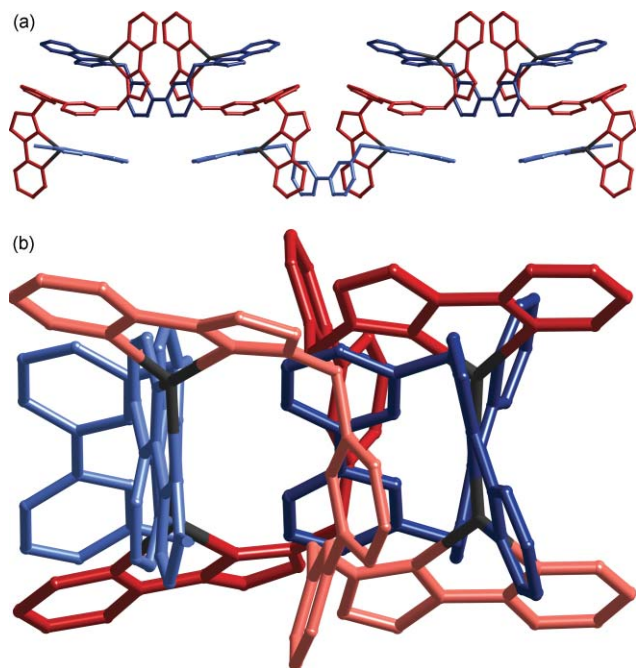
**Fig. 6** Asymmetric unit of $[\text{Ag}(\text{L}^{\text{biph}})(\text{BF}_4)(\text{Pr}_2\text{O})_{0.5}(\text{dmf})_{0.25}]_\infty$ showing the labelling scheme (H atoms, anions and solvent molecules omitted for clarity).

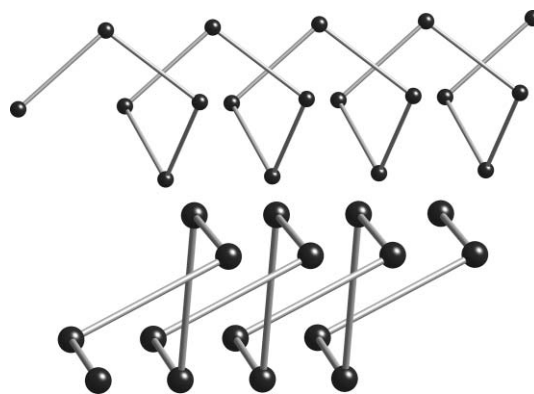
Table 5 Selected bond lengths (Å) and angles (°) for $[\text{Ag}(\text{L}^{\text{biph}})(\text{BF}_4)(^i\text{Pr}_2\text{O})_{0.5}(\text{dmf})_{0.25}]_{\infty}$

Ag(1)–N(61B)	2.306(8)	Ag(2)–N(21B)	2.271(7)
Ag(1)–N(61A)	2.309(8)	Ag(2)–N(21A)	2.288(7)
Ag(1)–N(51B)	2.332(8)	Ag(2)–N(11A)	2.344(7)
Ag(1)–N(51A)	2.335(7)	Ag(2)–N(11B)	2.369(8)
N(61B)–Ag(1)–N(61A)	127.4(3)	N(21B)–Ag(2)–N(21A)	131.7(2)
N(61B)–Ag(1)–N(51B)	72.5(3)	N(21B)–Ag(2)–N(11A)	140.8(2)
N(61A)–Ag(1)–N(51B)	129.9(3)	N(21A)–Ag(2)–N(11A)	72.2(2)
N(61B)–Ag(1)–N(51A)	146.9(3)	N(21B)–Ag(2)–N(11B)	71.8(3)
N(61A)–Ag(1)–N(51A)	71.9(3)	N(21A)–Ag(2)–N(11B)	133.1(2)
N(51B)–Ag(1)–N(51A)	118.4(3)	N(11A)–Ag(2)–N(11B)	117.6(3)

**Fig. 7** Two views of the chain in the structure of $[\text{Ag}(\text{L}^{\text{biph}})(\text{BF}_4)(^i\text{Pr}_2\text{O})_{0.5}(\text{dmf})_{0.25}]_{\infty}$. (a) A side-on view of the chain with crystallographically equivalent ligands coloured the same (red, dark blue, light blue). The ligands coloured red have no internal symmetry. The dark blue ligands (at the top of the picture) and the light blue ligands (bottom) each have twofold internal symmetry; thus the asymmetric unit contains two Ag(I) ions, one complete red ligand, and half of each of the light blue and dark blue ligands. (b) A view along a chain showing the relatively compact arrangement of the chain with no internal channel [cf. Fig 5(b)]; the dark red and light red ligands are crystallographically equivalent but are shaded differently for clarity. The light blue and dark blue ligands are crystallographically inequivalent, as before.

8.53 Å $[\text{Ag}(1) \cdots \text{Ag}(2)]$; and 7.67 Å $[\text{Ag}(2) \cdots \text{Ag}(2)]$. Although superficially similar to the structure of $[\text{Ag}(\text{L}^{\text{biph}})(\text{BF}_4)(\text{MeNO}_2)_{\infty}]$, the structure of $[\text{Ag}(\text{L}^{\text{biph}})(\text{BF}_4)(^i\text{Pr}_2\text{O})_{0.5}(\text{dmf})_{0.25}]_{\infty}$ has an important difference which is most apparent in the end-on view (Fig. 7b); there is no channel running along the centre of the chain because the conformation of the bridging ligands is such that the central space is occupied by the biphenyl spacers of the bridging ligands. The larger size of dmf molecules compared to nitromethane means that dmf molecules would be too big to occupy a channel like the one in $[\text{Ag}(\text{L}^{\text{biph}})(\text{BF}_4)(\text{MeNO}_2)_{\infty}]$, with the result that a more compact chain forms with the solvent molecules now in the spaces between the chains. The rectangular cross-section

of $[\text{Ag}(\text{L}^{\text{biph}})(\text{BF}_4)(^i\text{Pr}_2\text{O})_{0.5}(\text{dmf})_{0.25}]_{\infty}$ covers an area of ca. 14×10 Å, compared to ca. 17×17 Å for the nitromethane solvate in which the chain has a more open arrangement to allow solvent molecules to occupy a central channel. In addition, Fig. 8 shows the arrangement of Ag(I) ions along the axis of the chain in each structure. Whereas in $[\text{Ag}(\text{L}^{\text{biph}})(\text{BF}_4)(\text{MeNO}_2)_{\infty}]$ the sequence of Ag(I) ions forms an obvious helix with every Ag...Ag vector involving a rotational movement in the same sense about the axis of the chain, in $[\text{Ag}(\text{L}^{\text{biph}})(\text{BF}_4)(^i\text{Pr}_2\text{O})_{0.5}(\text{dmf})_{0.25}]_{\infty}$ this is not the case with alternate Ag...Ag vectors changing direction. Accordingly this latter chain is still chiral but is not helical.

**Fig. 8** The arrangement of Ag(I) ions in $[\text{Ag}(\text{L}^{\text{biph}})(\text{BF}_4)(\text{MeNO}_2)_{\infty}]$ (top) and $[\text{Ag}(\text{L}^{\text{biph}})(\text{BF}_4)(^i\text{Pr}_2\text{O})_{0.5}(\text{dmf})_{0.25}]_{\infty}$ (bottom), emphasising the more compact arrangement and the non-helical arrangement in the latter compared to the former.

The electrospray mass spectrum in each case indicates that the predominant species in solution is a dimer with peaks at 1239.2 $\{\text{Ag}_2(\text{L}^{\text{biph}})_2(\text{BF}_4)\}^+$ and 500.1 $\{\text{Ag}_2(\text{L}^{\text{biph}})_2\}^{2+}$. A weaker peak at 1903.4 $\{\text{Ag}_6(\text{L}^{\text{biph}})_6(\text{BF}_4)_4\}^{2+}$ suggests a small concentration of a higher oligomer, possibly a linear or cyclic polymer fragment. The ^1H NMR spectrum of $\{\text{Ag}(\text{L}^{\text{biph}})(\text{BF}_4)(\text{MeNO}_2)_{\infty}\}$ in acetonitrile shows peaks consistent with a two-fold symmetric ligand coordinated to Ag(I) at the pyrazolyl-pyridine groups. We suggest therefore that the solution species are likely to either be a fluxional dinuclear double helicate or a dinuclear mesocate. The ^1H NMR spectrum showed no changes on reducing the temperature to -40 °C.

Complex of Ag(I) with L^{mes} . The triangular ligand L^{mes} has been of particular interest in assembly of polyhedral cages with first-row transition metal dications because it caps a face of a metal cage, rather than spanning an edge; this recently allowed, for example, preparation of a cuboctahedral cage in which L^{mes} capped four of the eight triangular faces.^{5g} We expected that reaction with Ag(I) might, given the preference of Ag(I) for four-coordinate geometries, result in a trinuclear complex $[\text{Ag}_3(\text{L}^{\text{mes}})_2]^{3+}$ in which two ligands would cap opposite faces of an Ag_3 triangle; such M_3L_2 capsules based on other combinations of metal ions and triply-bridging ligands are well known.¹²

The material isolated from reaction of L^{mes} with AgBF_4 gave an ES mass spectrum showing peaks corresponding to $\text{Ag} : \text{L}^{\text{mes}}$ assemblies with 1 : 1, 2 : 2, 3 : 2, 2 : 3, 3 : 3 and 4 : 3 stoichiometries, suggesting a structure more complex than an $[\text{Ag}_3(\text{L}^{\text{mes}})_2]^{3+}$ cage. Recrystallisation afforded single crystals of coordination network $\{[\text{Ag}_4(\text{L}^{\text{mes}})_3](\text{BF}_4)_4\}_{\infty}$ with a slightly different ratio of components

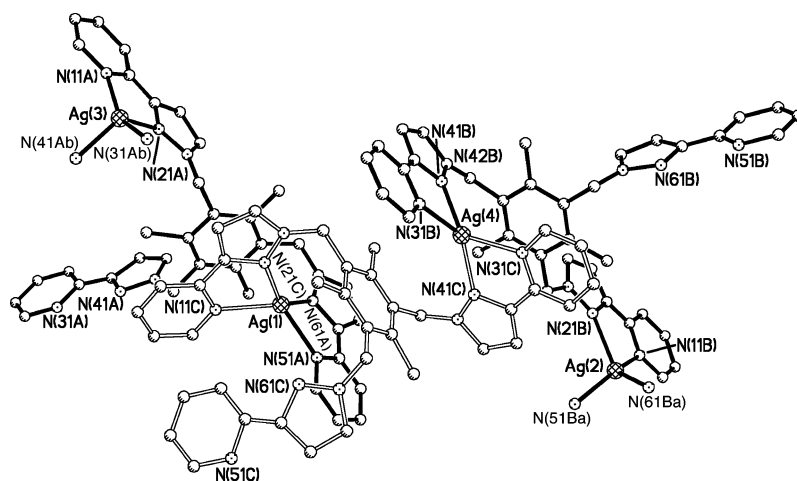


Fig. 9 Asymmetric unit of $\{[Ag_4(L^{mes})_3](BF_4)_4\}_\infty$ showing the labelling scheme (H atoms and anions omitted for clarity). One of the three independent ligands is shown with hollow bonds for clarity.

(Ag : L^{mes} = 1.33 : 1, rather than 1.5 : 1 which would occur in the cage) and in which Ag \cdots Ag interactions play an important role. It is likely that the high lability of Ag(I) permits a range of complexes with slightly different stoichiometries to be accessible, as others have noticed,¹³ and this network is the one that preferentially crystallises.

Crystals of $\{[Ag_4(L^{mes})_3](BF_4)_4\}_\infty$ were small and scattered very weakly, and required a synchrotron X-ray source to give a data set leading to a structure with $R_1 = 14.1\%$. The asymmetric unit contains four independent Ag(I) ions and three independent bridging ligands (Fig. 9 and 10, Table 6). Four Ag(I) ions require eight bidentate pyrazolyl-pyridine units, and the three ligands provide nine, so one pyrazolyl-pyridine unit is not involved in metal coordination. The Ag– L^{mes} assembly consists of a one-

Table 6 Selected bond lengths (Å) and angles (°) for $\{[Ag_4(L^{mes})_3](BF_4)_4\}_\infty$

Ag(1)–N(51A)	2.306(8)	Ag(1)–N(61A)	2.280(8)
Ag(1)–N(11C)	2.348(8)	Ag(1)–N(21C)	2.238(7)
Ag(2)–N(11B)	2.301(9)	Ag(2)–N(21B)	2.378(9)
Ag(2)–N(51B ^a)	2.350(9)	Ag(2)–N(61B ^a)	2.286(9)
Ag(3)–N(11A)	2.337(8)	Ag(3)–N(21A)	2.317(8)
Ag(3)–N(31A ^b)	2.364(8)	Ag(3)–N(41A ^b)	2.287(8)
Ag(4)–N(31B)	2.311(9)	Ag(4)–N(41B)	2.269(10)
Ag(4)–N(31C)	2.345(9)	Ag(4)–N(41C)	2.221(7)
N(51A)–Ag(1)–N(61A)	72.7(3)	N(51A)–Ag(1)–N(11C)	120.2(4)
N(51A)–Ag(1)–N(21C)	137.4(4)	N(61A)–Ag(1)–N(11C)	128.8(4)
N(61A)–Ag(1)–N(21C)	134.0(4)	N(11C)–Ag(1)–N(21C)	72.8(3)
Ag(3 ^c)–Ag(2)–N(11B)	81.0(3)	Ag(3 ^c)–Ag(2)–N(21B)	118.0(3)
Ag(3 ^c)–Ag(2)–N(51B ^a)	74.1(3)	Ag(3 ^c)–Ag(2)–N(61B ^a)	112.4(3)
N(11B)–Ag(2)–N(21B)	71.2(4)	N(11B)–Ag(2)–N(51B ^a)	153.8(4)
N(11B)–Ag(2)–N(61B ^a)	125.6(4)	N(21B)–Ag(2)–N(51B ^a)	113.5(4)
N(21B)–Ag(2)–N(61B ^a)	129.0(4)	N(51B ^a)–Ag(2)–N(61B ^a)	73.1(4)
Ag(2 ^d)–Ag(3)–N(11A)	76.6(2)	Ag(2 ^d)–Ag(3)–N(21A)	115.3(3)
Ag(2 ^d)–Ag(3)–N(31A ^a)	77.0(2)	Ag(2 ^d)–Ag(3)–N(41A ^b)	113.4(3)
N(11A)–Ag(3)–N(21A)	71.7(3)	N(11A)–Ag(3)–N(31A ^b)	152.5(3)
N(11A)–Ag(3)–N(41A ^a)	127.2(3)	N(21A)–Ag(3)–N(31A ^b)	113.9(3)
N(21A)–Ag(3)–N(41A ^a)	130.8(4)	N(31A ^b)–Ag(3)–N(41A ^b)	71.1(3)
N(31B)–Ag(4)–N(41B)	73.3(4)	N(31B)–Ag(4)–N(31C)	114.1(4)
N(31B)–Ag(4)–N(41C)	137.0(5)	N(41B)–Ag(4)–N(31C)	131.9(4)
N(41B)–Ag(4)–N(41C)	135.8(4)	N(31C)–Ag(4)–N(41C)	72.7(3)

Symmetry operations used to generate equivalent atoms^a $-x + 3, -y, -z$.
^b $-x + 1, -y + 1, -z + 1$. ^c $x + 1, y - 1, z$. ^d $x - 1, y + 1, z$.

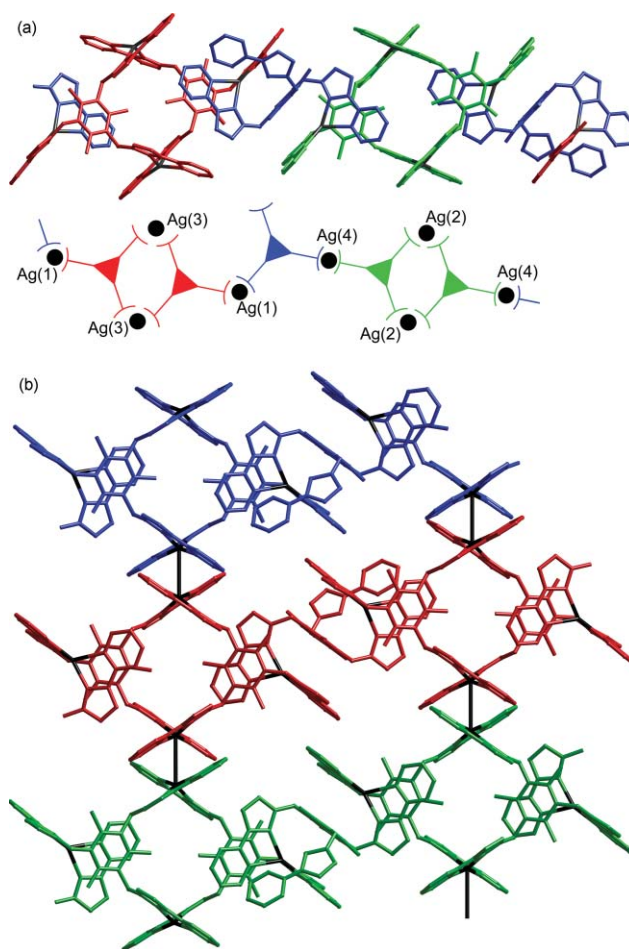


Fig. 10 Two views of the structure of $\{[Ag_4(L^{mes})_3](BF_4)_4\}_\infty$. (a) A view showing the chain structure, with crystallographically equivalent ligands coloured the same as each other; underneath is a sketch illustrating the connectivity. (b) A view showing the 2-D sheet formed by Ag \cdots Ag interactions between the chains; in this picture each chain has all of its ligands coloured the same (Ag atoms are in black).

dimensional chain whose basic connectivity is illustrated in Fig. 10(a), with symmetry-equivalent ligands in the same colour.

Thus the ligand repeat sequence is ABC–CBA–ABC–CBA *etc.* with the metal ions occurring along the chain either singly [Ag(1), Ag(4)] or in adjacent symmetry-equivalent pairs [Ag(2), Ag(3)]. The ligands depicted in red and green both use all three bidentate arms for coordination; the ligand depicted in blue has one of its three arms not coordinated to a metal ion. All four Ag(I) ions are accordingly coordinated by two bidentate N-donor units. These chains are further associated into two-dimensional sheets *via* Ag...Ag interactions involving Ag(2) and Ag(3) atoms in adjacent chains (separation 3.333 Å). The two pyrazolyl-pyridine units attached to each of these metal ions are also π -stacked with those from the other metal ion (see Fig. 10b); it will be apparent from this figure that columns of aromatic stacking between ligands run through the crystal structure.

Complexes of Hg(II) with L^{oPh} , L^{mPh} , L^{pPh} . Reaction of L^{oPh} with $Hg(ClO_4)_2$ in a 1 : 1 ratio in $MeNO_2$ afforded a clear solution from which a microcrystalline product deposited following diffusion of diethyl ether vapour into the solution. Given that other six-coordinate metal dications (Co^{2+} and Zn^{2+}) form tetrahedral $[M_4(L^{oPh})_6]^{8+}$ cages with L^{oPh} ,^{5a,5b} formation of an analogous cage seemed a likely possibility. However, the initially-formed crystalline material proved to be the simple mononuclear complex $[Hg(L^{oPh})](ClO_4)_2$ in which L^{oPh} acts as a tetradentate chelate to a single four-coordinate Hg(II) centre (Fig. 11, Table 7). The two HgN_2 planes make an angle of 46° to one another, and—as we have noted with other structures (see below)—the Hg–N(pyridyl) bonds are much shorter than the Hg–N(pyrazolyl) bonds, and the two

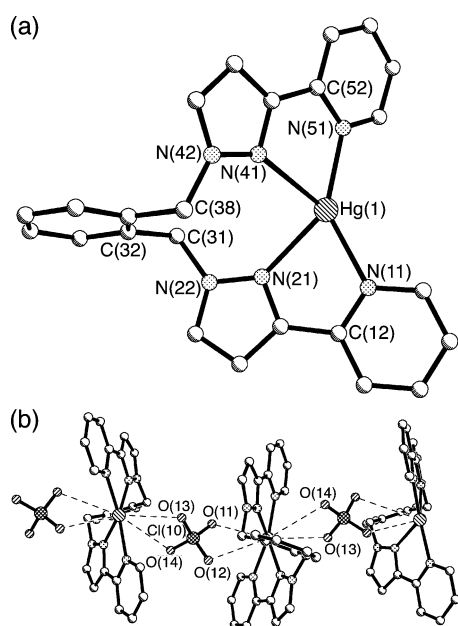


Fig. 11 Structure of the mononuclear complex $[Hg(L^{oPh})](ClO_4)_2$ (H atoms and one anion omitted for clarity).

Table 7 Selected bond lengths (Å) and angles ($^\circ$) for $[Hg(L^{oPh})](ClO_4)_2$

Hg(1)–N(51)	2.157(4)	Hg(1)–N(21)	2.342(4)
Hg(1)–N(11)	2.196(4)	Hg(1)–N(41)	2.458(4)
N(51)–Hg(1)–N(11)	139.96(15)	N(51)–Hg(1)–N(41)	72.95(14)
N(51)–Hg(1)–N(21)	145.48(15)	N(11)–Hg(1)–N(41)	136.97(14)
N(11)–Hg(1)–N(21)	72.75(16)	N(21)–Hg(1)–N(41)	87.40(14)

pyridyl donors subtend an angle of 140° at the Hg(II) centre. An N_4 pseudo-tetrahedral coordination environment is quite common in Hg(II) complexes.¹⁴ Oxygen atoms of one of the perchlorate anions are involved in weak pseudo-axial interactions to the metal ion [$Hg(1)\cdots O(11)$, 2.80 Å; $Hg(1)\cdots O(13)$, 2.90 Å; $Hg(1)\cdots O(12)$ and $Hg(1)\cdots O(14)$ are both > 3 Å] such that this perchlorate anion acts as a bridge linking chains of monomeric Hg(II) units (Fig. 11b).

On slower recrystallisation (weeks), however, we noticed that crystals of a different habit also formed; elemental analysis and mass spectrometry indicated the unexpected formulation $Hg_2(L)(ClO_4)_2$, consistent with formation of an Hg(I) species. The structure of $[Hg_2(L^{oPh})(MeNO_2)_2][ClO_4]_2$ (Fig. 12, Table 8) shows that a single ligand L^{oPh} can coordinate to an Hg_2^{2+} dimer with each pyrazolyl-pyridine group chelating one of the metal ions in a bidentate fashion, with the N_2Hg – HgN_2 core nearly planar: the two HgN_2 planes have an angle of 12° between them, and Hg(1) and Hg(2) are respectively 0.15 and 0.25 Å out of the mean plane of N(11), N(21), N(41) and N(51). The bridging phenylene unit is nearly perpendicular to the N_2Hg – HgN_2 core, making an angle of 81° with the N(11)–N(21)–N(41)–N(51) mean plane. The two Hg(I) centres are three-coordinate, with one bidentate N-donor chelating ligand [Hg–N distances 2.25–2.42 Å, with the Hg–N(pyridyl) bonds being shorter than the Hg–N(pyrazolyl) bonds] and an Hg...Hg bond (2.518 Å), although there are weak axial interactions with perchlorate oxygen atoms [$Hg(1)\cdots O(14)$, 2.89 Å; $Hg(2)\cdots O(13)$, 2.96 Å]. It is clear that the structure of L^{oPh} is ideally suited to holding a pair of Hg(I) ions together in an $\{Hg_2\}^{2+}$ unit, and this has facilitated slow reduction of Hg(II) to Hg(I) during the crystallisation.

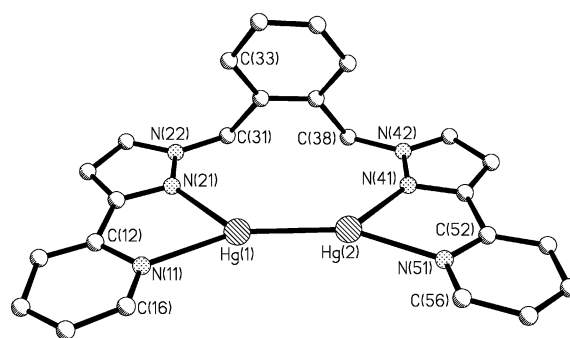


Fig. 12 Structure of the dinuclear complex cation of $[Hg_2(L^{oPh})(MeNO_2)_2][ClO_4]_2$ (H atoms omitted for clarity).

Reaction of L^{mPh} or L^{pPh} with $Hg(ClO_4)_2$ afforded, in the first instance, products assumed to be Hg(II) complexes. Mass spectroscopic analysis showed peaks corresponding to a wide range of Hg : L combinations and it seems likely that the initially-formed materials are either poorly-soluble coordination networks

Table 8 Selected bond lengths (Å) and angles ($^\circ$) for $[Hg_2(L^{oPh})(MeNO_2)_2][ClO_4]_2$

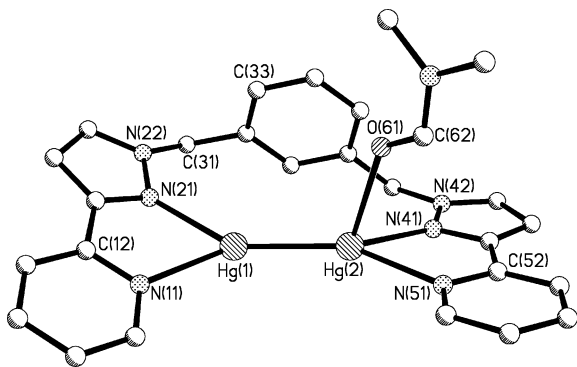
Hg(1)–N(11)	2.28(2)	N(11)–Hg(1)–N(21)	70.6(8)
Hg(1)–N(21)	2.42(2)	N(11)–Hg(1)–Hg(2)	155.7(5)
Hg(1)–Hg(2)	2.518(2)	N(21)–Hg(1)–Hg(2)	133.5(5)
Hg(2)–N(51)	2.25(2)	N(51)–Hg(2)–N(41)	71.1(8)
Hg(2)–N(41)	2.39(2)	N(51)–Hg(2)–Hg(1)	159.5(6)
		N(41)–Hg(2)–Hg(1)	126.7(5)

Table 9 Selected bond lengths (Å) and angles (°) for $[\text{Hg}_2(\text{L}^{\text{mPh}})(\text{DMF})_2][\text{ClO}_4]_2$

Hg(1)–Hg(2)	2.5237(6)	N(21)–Hg(1)–N(11)	70.09(19)
Hg(1)–N(21)	2.340(5)	N(21)–Hg(1)–Hg(2)	148.19(15)
Hg(1)–N(11)	2.354(6)	N(11)–Hg(1)–Hg(2)	138.43(14)
Hg(2)–N(51)	2.310(6)	N(51)–Hg(2)–N(41)	70.5(2)
Hg(2)–N(41)	2.373(6)	N(51)–Hg(2)–Hg(1)	149.56(15)
Hg(2)–O(61)	2.579(6)	N(41)–Hg(2)–Hg(1)	137.28(14)
		N(51)–Hg(2)–O(61)	79.56(19)
		N(41)–Hg(2)–O(61)	90.7(2)
		Hg(1)–Hg(2)–O(61)	107.16(13)

or mixtures of products. NMR spectra of these materials showed them clearly to be complicated mixtures. If the Hg(II) ions are four-coordinate, one-dimensional coordination chains are likely products (*cf.* some of the Ag(I) complexes described earlier); if they are six-coordinate, cage complexes are the likely result.^{5g,5h} However, slow recrystallisation (weeks) again afforded in each case, in modest yield, a crop of X-ray quality single crystals for which elemental analysis indicated the formulation $\text{Hg}_2(\text{L})(\text{ClO}_4)_2$; this was confirmed crystallographically. As before we assume that very slow reduction of Hg(II) to Hg(I) allows good quality crystals to be formed.

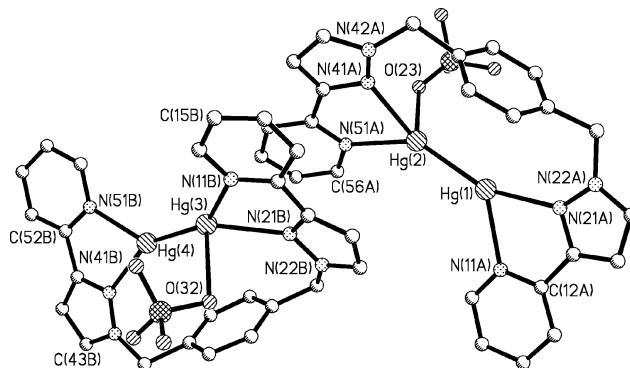
$[\text{Hg}_2(\text{L}^{\text{mPh}})(\text{dmf})_2][\text{ClO}_4]_2$ displays essentially the same core structure as $[\text{Hg}_2(\text{L}^{\text{pPh}})]^{2+}$, with the two Hg(I) ions in distorted trigonal planar coordination environments having Hg–N bond lengths in the slightly narrower range 2.31–2.37 Å, and an Hg–Hg separation of 2.524 Å (Fig. 13, Table 9). The $\text{N}_2\text{Hg}–\text{HgN}_2$ core is considerably more distorted from planarity, with a twist of 18° between the two HgN_2 planes. Whereas Hg(1) is three coordinate, Hg(2) has an additional axial interaction with a dmf solvent molecule $[\text{Hg}(2) \cdots \text{O}(61), 2.579 \text{ Å}]$.

**Fig. 13** Structure of the dinuclear complex cation of $[\text{Hg}_2(\text{L}^{\text{mPh}})(\text{dmf})_2][\text{ClO}_4]_2$ (H atoms omitted for clarity).

The crystal structure of $[\text{Hg}_2(\text{L}^{\text{pPh}})][\text{ClO}_4]_2$ contains in the asymmetric unit two independent but similar $[\text{Hg}_2(\text{L}^{\text{pPh}})][\text{ClO}_4]_2$ units, each having the same basic dinuclear structure as in the previous examples but with a slightly different conformation from each other (Fig. 14, Table 10). All four Hg(I) ions are in a distorted trigonal planar coordination environment with Hg–N bond lengths in the range 2.26–2.42 Å and Hg–Hg separations of 2.52 Å. In the molecule containing Hg(1) and Hg(2) the two HgN_2 planes have a twist of 30° between them, and both metal ions have weak axial interactions with perchlorate ions which are on opposite faces of the $\text{N}_2\text{Hg}–\text{HgN}_2$ unit to minimise steric interference between them $[\text{Hg}(1) \cdots \text{O}(11), 2.729 \text{ Å}; \text{Hg}(2) \cdots \text{O}(23), 2.656 \text{ Å}]$. The second

Table 10 Selected bond lengths (Å) and angles (°) for $[\text{Hg}_2(\text{L}^{\text{pPh}})][\text{ClO}_4]_2$

Hg(1)–Hg(2)	2.5227(7)	N(21A)–Hg(1)–N(11A)	70.9(3)
Hg(1)–N(21A)	2.259(8)	N(21A)–Hg(1)–Hg(2)	158.43(19)
Hg(1)–N(11A)	2.398(8)	N(11A)–Hg(1)–Hg(2)	130.7(2)
Hg(2)–N(51A)	2.322(8)	N(51A)–Hg(2)–N(41A)	70.8(3)
Hg(2)–N(41A)	2.390(8)	N(51A)–Hg(2)–Hg(1)	143.5(2)
		N(41A)–Hg(2)–Hg(1)	137.3(2)
Hg(3)–Hg(4)	2.5149(8)	N(11B)–Hg(3)–N(21B)	71.1(3)
Hg(3)–N(11B)	2.279(8)	N(11B)–Hg(3)–Hg(4)	148.9(2)
Hg(3)–N(21B)	2.421(8)	N(21B)–Hg(3)–Hg(4)	138.6(2)
Hg(4)–N(41B)	2.295(8)	N(41B)–Hg(4)–N(51B)	70.9(3)
Hg(4)–N(51B)	2.340(8)	N(41B)–Hg(4)–Hg(3)	150.7(2)
		N(51B)–Hg(4)–Hg(3)	137.79(19)

**Fig. 14** Structure of the two independent dinuclear complex units of $[\text{Hg}_2(\text{L}^{\text{pPh}})][\text{ClO}_4]_2$ (H atoms omitted for clarity).

molecule is even more distorted with a twist between the two HgN_2 planes of 45°; again there are weak axial interactions with perchlorate ions $[\text{Hg}(3) \cdots \text{O}(32), 2.830 \text{ Å}; \text{Hg}(4) \cdots \text{O}(42), 2.818 \text{ Å}]$. The two independent complex cations are associated by a π -stacking interaction involving one pyrazolyl-pyridine unit of each cation. The Hg \cdots Hg separations are 2.523 Å $[\text{Hg}(1) \cdots \text{Hg}(2)]$ and 2.515 Å $[\text{Hg}(3) \cdots \text{Hg}(4)]$.

This set of Hg(I) complexes with L^{pPh} , L^{mPh} or L^{Ph} forms an interesting homologous series. Whilst other examples of Hg_2^{2+} dimers with $\text{N}_2\text{Hg}–\text{HgN}_2$ donor sets are known,¹⁵ they are very much rarer than Hg(II) complexes.^{7,16} It is suggested that the driving force for these cation–cation interactions is the large increase in solvation energy on moving from a mono- to di-cation arising from a quadratic dependence on the charge of the species.¹⁷ It is noticeable how L^{pPh} appears to have an optimal separation between the two bidentate groups to accommodate an Hg_2^{2+} unit with the ligand in a near-planar conformation; as the ligands get longer, due to the *meta* and then *para* substitution pattern of the bridging ligand, greater degrees of distortion are required to bring the two bidentate termini close enough together to accommodate the Hg_2^{2+} unit. It is also apparent that the Hg \cdots Hg separation does not have much scope for variation, being $\approx 2.52 \text{ Å}$ in every case.

For all three complexes, ES mass spectra in dmf solution confirm retention of the dinuclear complex with its Hg \cdots Hg interaction, with peaks at m/z 893.1 $\{[\text{Hg}_2(\text{L})(\text{ClO}_4)]^+\}$ and 397.1 $\{[\text{Hg}_2(\text{L})]^{2+}$ (where $\text{L} = \text{L}^{\text{pPh}}$, L^{mPh} or L^{Ph}) in each case. A number of other peaks in the mass spectrum suggest the presence of several other species including $[\text{Hg}(\text{L})_2][\text{ClO}_4]$, $[\text{Hg}_2(\text{L})_2][\text{ClO}_4]_2$ and $[\text{Hg}_2(\text{L})_2][\text{ClO}_4]_4$. It is therefore likely that the structure observed in the solid state

is in each case a kinetic crystallisation product of a mixture of several species in solution.

Tetrahedral cage complex of Hg(II) with L^{biph}. The formation of the dinuclear Hg(II) complexes described above is clearly facilitated by the fact that the ligands L^{mPh} and L^{pPh} are sufficiently short to be able to coordinate one bidentate terminus to each Hg(II) centre of the {Hg₂}²⁺ unit. We were therefore interested to see what would happen using a much longer bridging ligand, such as L^{biph}, where this cannot happen as the two pyrazolyl-pyridine units are too far apart. The reaction of L^{biph} with Hg(ClO₄)₂ in a 1 : 1 ratio in nitromethane gave a colourless solution from which crystals were grown by the slow diffusion of diisopropyl ether. Elemental analysis of the crystals suggested the empirical formula Hg₄(L^{biph})₃(ClO₄)₄, indicating that in this case the metal ions have remained in the +2 oxidation state. The crystal structure shows the complex to be the tetrahedral cage [Hg₄(L^{biph})₆ClO₄][ClO₄]₇·(MeNO₂)₃ (Fig. 15, Table 11). Four six-

Table 11 Selected bond lengths (Å) for [Hg₄(L^{biph})₆ClO₄][ClO₄]₇·(MeNO₂)₃

Hg(1)–N(21C)	2.306(15)	Hg(3)–N(11E)	2.196(12)
Hg(1)–N(21A)	2.327(12)	Hg(3)–N(61D)	2.308(12)
Hg(1)–N(11B)	2.340(15)	Hg(3)–N(51D)	2.398(12)
Hg(1)–N(11A)	2.375(14)	Hg(3)–N(51B)	2.485(12)
Hg(1)–N(21B)	2.432(13)	Hg(3)–N(21E)	2.495(13)
Hg(1)–N(11C)	2.487(12)	Hg(3)–N(61B)	2.512(14)
Hg(2)–N(61F)	2.268(12)	Hg(4)–N(11F)	2.262(14)
Hg(2)–N(11D)	2.272(13)	Hg(4)–N(61E)	2.301(13)
Hg(2)–N(21D)	2.390(12)	Hg(4)–N(21F)	2.438(14)
Hg(2)–N(51A)	2.442(11)	Hg(4)–N(61C)	2.451(11)
Hg(2)–N(51F)	2.449(11)	Hg(4)–N(51C)	2.471(12)
Hg(2)–N(61A)	2.477(13)	Hg(4)–N(51E)	2.476(14)

coordinate Hg(II) ions lie at the corners of the tetrahedron and are each coordinated by a bidentate terminus from three of the six ligands which span each of the edges of the cage. One of the eight ClO₄[−] anions is encapsulated inside the cage. The topology of the cage is similar to that of the previously described series of Co(II) cages [Co₄(L^{biph})₆CA][A]₇ (A[−] = BF₄[−], ClO₄[−], PF₆[−] and I[−]).^{5e} Clearly, the fact that L^{biph} is too long to coordinate both bidentate termini to the same metal centre precludes formation of either simple mononuclear complexes {cf. [Hg(L^{oPh})](ClO₄)₂} or the dinuclear Hg(II) complexes.

The Hg–N bond lengths are in the range 2.20–2.50 Å, slightly longer than those for HgN₄ donor sets and similar to other examples of HgN₆ coordination.¹⁸ The tetrahedron is more regular than those observed for cages with Co(II);^{5e} the Hg...Hg separations along the edges of the tetrahedron span the narrower range 11.64–12.23 Å. There are two types of metal coordination geometry present in the cage; Hg(1) has *fac* tris-chelate geometry, whereas the remaining three Hg(II) ions have *mer* tris-chelate geometry. This results in the cage having a (non-crystallographic) C₃ symmetry axis through Hg(1) and the centre of the triangular face defined by Hg(2)–Hg(3)–Hg(4), such that all three ligands in the basal plane are equivalent, and the three ligands connecting the base to the apex are equivalent, with neither type of ligand having any internal symmetry. All the metal centres in each cage have the same optical configuration, all Δ or all Λ with both enantiomers present in the unit cell.

As observed for the Co(II) analogues, the encapsulated ClO₄[−] anion is closer to ‘apical’ Hg(1) (Hg...Cl: 5.85 Å) than the three ‘basal’ Hg(II) ions (Hg...Cl separations in the range 7.81–7.95 Å). This displacement allows the oxygen atoms of the ClO₄[−] to make several contacts with the CH₂ linker units short enough to be C–H...O hydrogen bonds (O...C distances 3.09–3.24 Å). Three more anions outside the cage sit in cavities in the three faces of the tetrahedron which meet at Hg(1), and make similar C–H...O hydrogen bonds with CH₂ groups from the ligands.

Intramolecular π–π stacking interactions are an important feature of the complex; every single pyrazolyl-pyridine group is π-stacked to the phenyl ring of a neighbouring ligand’s spacer unit (separations 3.2–3.7 Å). Twists between the rings of the biphenyl spacers allow each phenyl ring to optimise these interactions by aligning itself better with the adjacent pyrazolyl-pyridine units. These twist angles between phenyl rings are larger for the ligands connected to ‘apical’ Hg(1) (42.6–52.7°) than for the ligands spanning the ‘basal’ Hg(II) ions (26.2–30.6°). Outside the cage the remaining four perchlorate anions, and solvent molecule, were

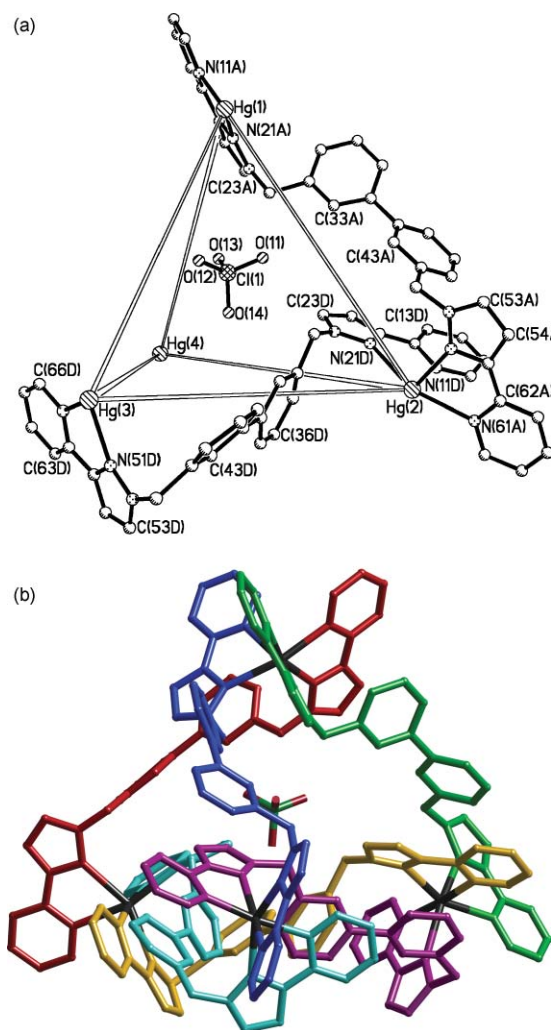


Fig. 15 Two views of the complex cation of the cage complex [Hg₄(L^{biph})₆ClO₄][ClO₄]₇·(MeNO₂)₃ (H atoms and all anions except the encapsulated one omitted for clarity). (a) A view emphasising the tetrahedral architecture, showing two ligands and part of the numbering scheme. (b) A view showing the whole cage with each ligand coloured separately.

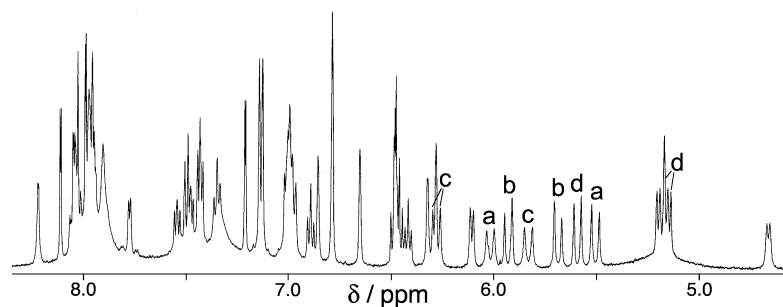


Fig. 16 500 MHz ^1H NMR spectrum of $[\text{Hg}_4(\text{L}^{\text{biph}})_6\text{C}(\text{ClO}_4)]_7$, showing the presence of two independent ligand environments (as observed in the crystal structure); the eight protons of the four CH_2 groups were matched into pairs (labelled a–d) with a COSY spectrum.

difficult to locate with only limited data from weakly scattering crystals. They are distributed over several disordered sites with fractional occupancies, though the approximate overall total of eight anions, which confirms the oxidation state of the $\text{Hg}(\text{II})$ ions, is clear. The ^1H NMR spectrum of the complex (Fig. 16) is exactly consistent with the cage structure observed in the solid state being retained in solution, with signals in the aromatic region totalling 48 protons (from two inequivalent ligands which have no internal symmetry). Although many of the signals are overlapping, enough of them are distinct to allow accurate integration; of particular note are the eight doublets with the lowest chemical shift which correspond to the protons of the four inequivalent CH_2 groups (confirmed by a two-dimensional COSY spectrum). The fact that this NMR spectrum is clean, with no indication of minor additional components or traces of free ligand, indicates that the cage complex is a robust structure which completely retains its integrity in solution—an important point from the view of future studies into its host–guest chemistry.

Helical and catenated trinuclear complexes of $\text{Hg}(\text{II})$ with L^{232} .

We described earlier how L^{232} formed trinuclear double helicates with a range of metal ions, including a mixed-metal $\text{Ag}(\text{I})$ – $\text{Fe}(\text{II})$ – $\text{Ag}(\text{I})$ complex exploiting the four-coordinate and six-coordinate nature of the terminal and central binding sites in the helicate.^{5f} Reaction of L^{232} with $\text{Hg}(\text{ClO}_4)_2$ afforded a mixture of two crystalline products which could be separated manually. The major product is the trinuclear helicate $[\text{Hg}_3(\text{L}^{232})_2](\text{ClO}_4)_6 \cdot 6\text{MeCN}$ in which all three metal centres are in the same $\text{Hg}(\text{II})$ oxidation state despite their different coordination environments (Fig. 17, Table 12). The central ion $\text{Hg}(2)$, although nominally six-coordinate, displays

Hg – N separations in the range from 2.277–2.614 Å with the shortest two being to the pair of pyridyl donors which are mutually *trans*; the Hg – N (pyrazolyl) donors are all considerably longer, and the average Hg – N distance is 2.42 Å. In contrast the terminal ions $\text{Hg}(1)$ and $\text{Hg}(3)$ both have four-coordinate environments in which the $\text{N}(\text{pyridyl})$ – Hg – $\text{N}(\text{pyridyl})$ angle is close to linear [174° at $\text{Hg}(1)$ and 158° at $\text{Hg}(3)$] and these bonds are relatively short, with the Hg – N (pyrazolyl) bonds again being much longer.

Table 12 Selected bond lengths (Å) for $[\text{Hg}_3(\text{L}^{232})_2](\text{ClO}_4)_6 \cdot 6\text{MeCN}$

$\text{Hg}(1)$ – $\text{N}(11\text{B})$	2.151(4)	$\text{Hg}(3)$ – $\text{N}(91\text{A})$	2.155(3)
$\text{Hg}(1)$ – $\text{N}(11\text{A})$	2.162(4)	$\text{Hg}(3)$ – $\text{N}(91\text{B})$	2.238(4)
$\text{Hg}(1)$ – $\text{N}(21\text{A})$	2.404(4)	$\text{Hg}(3)$ – $\text{N}(81\text{B})$	2.307(4)
$\text{Hg}(1)$ – $\text{N}(21\text{B})$	2.488(4)	$\text{Hg}(3)$ – $\text{N}(81\text{A})$	2.442(4)
$\text{Hg}(2)$ – $\text{N}(51\text{A})$	2.277(3)	$\text{Hg}(2)$ – $\text{N}(41\text{A})$	2.412(3)
$\text{Hg}(2)$ – $\text{N}(51\text{B})$	2.286(3)	$\text{Hg}(2)$ – $\text{N}(41\text{B})$	2.531(3)
$\text{Hg}(2)$ – $\text{N}(61\text{B})$	2.373(3)	$\text{Hg}(2)$ – $\text{N}(61\text{A})$	2.614(3)
$\text{N}(11\text{B})$ – $\text{Hg}(1)$ – $\text{N}(11\text{A})$	174.46(15)	$\text{N}(91\text{A})$ – $\text{Hg}(3)$ – $\text{N}(91\text{B})$	157.94(13)
$\text{N}(11\text{B})$ – $\text{Hg}(1)$ – $\text{N}(21\text{A})$	110.19(13)	$\text{N}(91\text{A})$ – $\text{Hg}(3)$ – $\text{N}(81\text{B})$	125.46(13)
$\text{N}(11\text{A})$ – $\text{Hg}(1)$ – $\text{N}(21\text{A})$	73.91(13)	$\text{N}(91\text{B})$ – $\text{Hg}(3)$ – $\text{N}(81\text{B})$	73.66(13)
$\text{N}(11\text{B})$ – $\text{Hg}(1)$ – $\text{N}(21\text{B})$	73.34(13)	$\text{N}(91\text{A})$ – $\text{Hg}(3)$ – $\text{N}(81\text{A})$	74.34(13)
$\text{N}(11\text{A})$ – $\text{Hg}(1)$ – $\text{N}(21\text{B})$	108.52(13)	$\text{N}(91\text{B})$ – $\text{Hg}(3)$ – $\text{N}(81\text{A})$	105.15(13)
$\text{N}(21\text{A})$ – $\text{Hg}(1)$ – $\text{N}(21\text{B})$	116.35(12)	$\text{N}(81\text{B})$ – $\text{Hg}(3)$ – $\text{N}(81\text{A})$	124.30(12)
$\text{N}(51\text{A})$ – $\text{Hg}(2)$ – $\text{N}(51\text{B})$	159.61(12)	$\text{N}(61\text{B})$ – $\text{Hg}(2)$ – $\text{N}(41\text{B})$	139.83(12)
$\text{N}(51\text{A})$ – $\text{Hg}(2)$ – $\text{N}(61\text{B})$	124.77(12)	$\text{N}(41\text{A})$ – $\text{Hg}(2)$ – $\text{N}(41\text{B})$	114.62(11)
$\text{N}(51\text{B})$ – $\text{Hg}(2)$ – $\text{N}(61\text{B})$	70.68(12)	$\text{N}(51\text{A})$ – $\text{Hg}(2)$ – $\text{N}(61\text{A})$	69.48(12)
$\text{N}(51\text{A})$ – $\text{Hg}(2)$ – $\text{N}(41\text{A})$	71.23(12)	$\text{N}(51\text{B})$ – $\text{Hg}(2)$ – $\text{N}(61\text{A})$	93.89(11)
$\text{N}(51\text{B})$ – $\text{Hg}(2)$ – $\text{N}(41\text{A})$	126.80(12)	$\text{N}(61\text{B})$ – $\text{Hg}(2)$ – $\text{N}(61\text{A})$	108.24(11)
$\text{N}(61\text{B})$ – $\text{Hg}(2)$ – $\text{N}(41\text{A})$	85.45(12)	$\text{N}(41\text{A})$ – $\text{Hg}(2)$ – $\text{N}(61\text{A})$	139.18(11)
$\text{N}(51\text{A})$ – $\text{Hg}(2)$ – $\text{N}(41\text{B})$	95.17(11)	$\text{N}(41\text{B})$ – $\text{Hg}(2)$ – $\text{N}(61\text{A})$	79.76(11)
$\text{N}(51\text{B})$ – $\text{Hg}(2)$ – $\text{N}(41\text{B})$	69.52(12)		

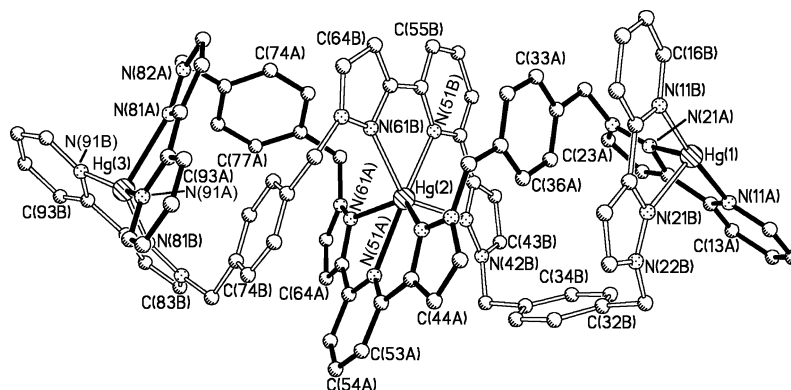


Fig. 17 Structure of the complex cation of the trinuclear double helicate $[\text{Hg}_3(\text{L}^{232})_2](\text{ClO}_4)_6 \cdot 6\text{MeCN}$ (H atoms omitted for clarity).

The average Hg–N distances are 2.30 Å for Hg(1) and 2.29 Å at Hg(3), with the shorter average bond length [compared to Hg(1)] reflecting the lower coordination number. The intertwining of the two ligands results in inter-ligand π -stacking, with each ligand having one of its phenylene spacers stacked between two pyrazolyl/pyridine units of the other ligand. This phenylene spacer also has two of its C–H bonds directed towards the face of a phenylene spacer from the other ligand to which it is near-perpendicular [87° between rings C(72A)–C(77A) and C(72B)–C(77B); and 83° between rings C(32A)–C(37A) and C(32B)–C(37B)], resulting in a combination of face-to-face and edge-to-face stacking involving these phenylene spacers. Despite the fact that, in the crystal structure, the two phenylene spacers of each ligand are in quite distinct environments (one in the helical ‘core’ involved in π -stacking, and one on the periphery of the helix), the ¹H NMR spectrum in solution shows a symmetric structure with each ligand having twofold symmetry (see Experimental). The Hg(1)···Hg(2) and Hg(2)···Hg(3) separations are 7.89 and 7.63 Å respectively.

The minor product from this reaction proved to be something of a surprise and is shown in Fig. 18, Table 13; it is a catenate [Hg₃(L^{232-H})₂](ClO₄)₄·3MeNO₂ in which each mono-deprotonated ligand forms an independent macrocyclic ring by coordination of its termini to the *same* Hg(II) ion, with the two metallo-macrocyclic rings connected by a third Hg(II) ion bound to the terdentate unit of each ligand. This assembly therefore achieves the same 3 : 2 metal : ligand stoichiometry but in a different way from that found in the helicate in which all three binding sites of

each ligand interact with a different metal ion. An additional and unexpected feature of this is that each of the terminal Hg(II) ions is coordinated to a pyrazolyl ring in a cyclometallating C-donor coordination mode; cyclometallating coordination of aromatic ligands to Hg(II) is well known.¹⁹ Thus the central metal ion Hg(1) is in an N₆ coordination environment with, again, the two shortest bonds being those to the pyridyl donors. The terminal metal ions Hg(2) and Hg(3) are however each coordinated by one pyrazolyl-pyridine unit from the terminus of one ligand, and a cyclometallating pyrazolyl donor from the other terminus of

Table 13 Selected bond lengths (Å) and angles (°) for [Hg₃(L^{232-H})₂](ClO₄)₄·3MeNO₂

Hg(1)–N(51A)	2.294(8)	Hg(2)–C(84A)	2.024(11)
Hg(1)–N(51B)	2.315(8)	Hg(2)–N(11A)	2.130(10)
Hg(1)–N(41B)	2.348(8)	Hg(2)–N(21A)	2.680(9)
Hg(1)–N(41A)	2.363(8)	Hg(3)–C(84B)	2.040(11)
Hg(1)–N(61B)	2.486(8)	Hg(3)–N(11B)	2.124(10)
Hg(1)–N(61A)	2.526(8)	Hg(3)–N(21B)	2.642(9)
N(51A)–Hg(1)–N(51B)	155.1(3)	N(51B)–Hg(1)–N(61A)	91.5(3)
N(51A)–Hg(1)–N(41B)	126.1(3)	N(41B)–Hg(1)–N(61A)	98.8(3)
N(51B)–Hg(1)–N(41B)	70.7(3)	N(41A)–Hg(1)–N(61A)	139.0(3)
N(51A)–Hg(1)–N(41A)	70.5(3)	N(61B)–Hg(1)–N(61A)	96.1(3)
N(51B)–Hg(1)–N(41A)	129.4(3)	C(84A)–Hg(2)–N(11A)	171.6(5)
N(41B)–Hg(1)–N(41A)	98.4(3)	C(84A)–Hg(2)–N(21A)	116.5(4)
N(51A)–Hg(1)–N(61B)	97.1(3)	N(11A)–Hg(2)–N(21A)	70.2(4)
N(51B)–Hg(1)–N(61B)	68.6(3)	C(84B)–Hg(3)–N(11B)	174.0(4)
N(41B)–Hg(1)–N(61B)	136.8(3)	C(84B)–Hg(3)–N(21B)	113.7(4)
N(41A)–Hg(1)–N(61B)	96.3(3)	N(11B)–Hg(3)–N(21B)	70.7(3)
N(51A)–Hg(1)–N(61A)	69.2(3)		

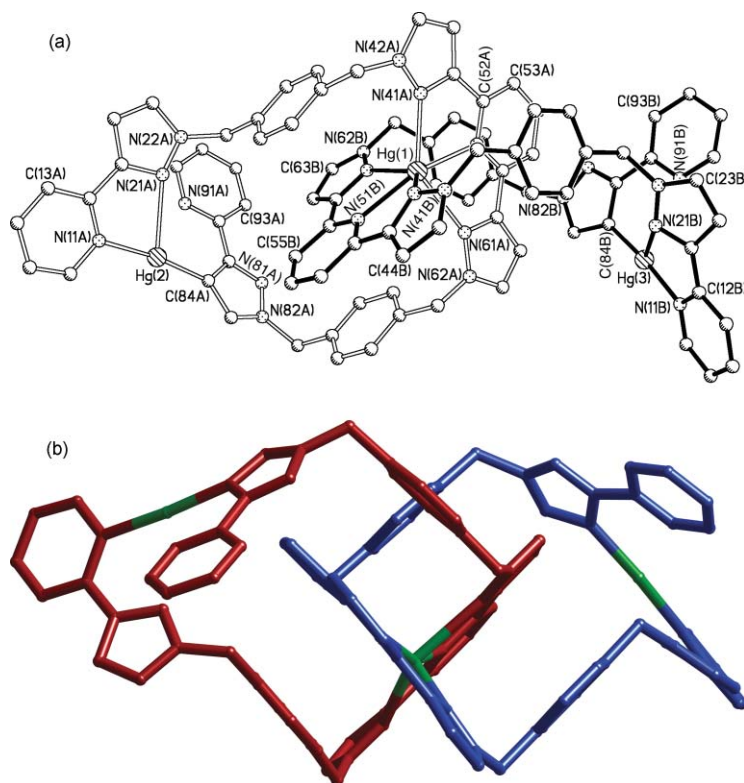


Fig. 18 Two views of the complex cation of the trinuclear cyclometallated catenate [Hg₃(L^{232-H})₂](ClO₄)₄·3MeNO₂ (H atoms omitted for clarity). (a) A view showing the atom labelling scheme, with one ligand depicted with hollow bonds for clarity; (b) a view emphasising the aromatic stacking around the central Hg(II) ion.

the *same* ligand. The coordination geometry around Hg(2) and Hg(3) is in fact nearly linear two-coordinate [from pyridyl *N* and pyrazolyl *C* donors subtending an angle of 172° at Hg(2) and 174° at Hg(3)] with the Hg–N(pyrazolyl) distances being much longer (2.68 and 2.64 Å respectively). A significant feature of the structures is aromatic π -stacking, with the terdentate bis(pyrazolyl)-pyridine unit of each ligand sandwiched between the two *para*-phenylene groups of the other with separations of \approx 3.4–3.5 Å between the near-parallel planes. ES mass spectra of a redissolved crystal confirmed retention of the structure in solution, with peaks apparent at *m/z* 1105.2, 703.5 and 502.6 corresponding to $\{\text{Hg}_3(\text{L}^{232}_{-\text{H}})_2(\text{ClO}_4)_n\}^{(4-n)+}$ ($n = 2, 1, 0$ respectively). We were unable to isolate enough crystals for a good ^1H NMR spectrum. We could not convert the helicate $[\text{Hg}_3(\text{L}^{232})_2](\text{ClO}_4)_6$ to the catenate $[\text{Hg}_3(\text{L}^{232}_{-\text{H}})_2](\text{ClO}_4)_4$ by treatment with base, even under vigorous conditions (prolonged reflux in MeNO_2), presumably the catenate forms by an alternative pathway and once the helicate has formed it is kinetically quite stable.

Preparation of catenates based on metal-ion template effects is a popular theme in supramolecular coordination chemistry,²⁰ and several rational syntheses have been reported since the first examples from Sauvage *et al.* based on the Cu(I)/phen skeleton.²¹ The formation of a catenated structure here, albeit as a minor component during formation of the trinuclear helicate, likely occurs only because for Hg(II) a cyclometallated coordination mode is possible. (We note that Sauvage *et al.* reported a mononuclear catenate based on unexpected C–H activation of an aromatic ring by Pd(II), giving a cyclometallated structure, in 1989).²² Examination of the structure of $[\text{Hg}_3(\text{L}^{232}_{-\text{H}})_2](\text{ClO}_4)_4$ suggests that conventional *N,N*-bidentate coordination of the two terminal pyrazolyl-pyridine units of each ligand to the same terminal metal centre would be difficult in a catenated structure, as the two arms of each ligand cannot stretch far enough to converge to the necessary extent to provide an N_4 coordination environment. In fact only one pyrazolyl *N*-donor interacts with each terminal Hg(II) centre and those are weak, long-range interactions; the principal coordination to these Hg(II) centres is the near-linear *N,C* (pyridine and cyclometallated pyrazolyl) donors. Cyclometallation to Hg(II) is favoured when the coordination number is low, as here, because of the electroneutrality principle;¹⁹ anionic *C*-donor ligands would make the metal centre too electron rich if there were too many other ligands. Accordingly with metal ions such as first-row transition metals and Ag(I), where cyclometallation as a coordination mode is rarer, only the conventional trinuclear helicates were observed on reaction with L^{232} with no evidence for alternative cyclometallated products.^{5j}

Conclusions

This set of ligands has afforded an interesting range of structural types in the complexes with Ag(I), Hg(I) and Hg(II). Four-coordinate bis-bidentate coordination around Ag(I) can afford a dinuclear double helicate, a dinuclear mesocate or an infinite one-dimensional chain from a set of three very similar bridging ligands (L^{mPh} , L^{mTol} and L^{pPh}). With the more extended bridging ligand L^{biph} one-dimensional chains result whose conformation depends on whether or not solvent molecules can be accommodated in a channel along the core of the chain. The triply-bridging ligand L^{mes} appears to afford the simple cage $[\text{Ag}_3(\text{L}^{\text{mes}})_2]^{2+}$ in solution, but

crystallisation affords a complex two-dimensional coordination polymer in which Ag \cdots Ag interactions play an important role in cross-linking adjacent one-dimensional chains.

The coordination chemistry of these ligands with mercury is complicated by the availability of two oxidation states: L^{pPh} , L^{mPh} and L^{pPh} all afford $[\text{Hg}_2\text{L}]^{2+}$ based on an $\{\text{Hg}^{\text{I}}_2\}^{2+}$ metal–metal bonded core with one end of the bridging ligand attached to each metal ion. Where reduction to Hg(I) did not occur, the Hg(II) centres could be either four-coordinate {as in mononuclear $[\text{Hg}(\text{L}^{\text{pPh}})]^{2+}$ } or six-coordinate {as in the tetranuclear cage $[\text{Hg}_4(\text{L}^{\text{biph}})_6\text{ClO}_4]^{7+}$ which contains an anion in the central cavity}. Both four- and six-coordinate Hg(II) centres occur in the trinuclear double helicate $[\text{Hg}_3(\text{L}^{232})_2]^{6+}$. Finally, a surprise by-product in the preparation of $[\text{Hg}_3(\text{L}^{232})_2]^{6+}$ was the catenate $[\text{Hg}_3(\text{L}^{232}_{-\text{H}})_2]^{4+}$ whose formation is made possible by the facility with which Hg(II) forms cyclometallated complexes having low coordination numbers. For the Hg compounds in particular, the possibility of Hg^I–Hg^I metal–metal bonded species forming, and the possibility of cyclometallation of a pyrazolyl ring, result in highly unpredictable coordination chemistry.

Experimental

General details

The ligands L^{mPh} ,^{5h} L^{pPh} ,^{5g} and L^{biph} (ref. 5e) were prepared as described previously. Other organic starting materials and metal salts were purchased from Aldrich and used as received. ^1H NMR spectra were recorded on Bruker AC-250, AMX2-400 or DRX-500 spectrometers. Electron impact mass spectra were recorded on a VG-Autospec magnetic sector instrument at the University of Sheffield. Electrospray mass spectra were recorded on a VG Quattro II triple-quadrupole instrument or a Bruker MicroTOF mass spectrometer in electrospray positive ion mode, at the University of Huddersfield.

Preparation of L^{mTol}

N-Bromo-succinimide (42 g, 233.2 mmol) and AIBN (*ca.* 5 mg) were added to a stirred solution of mesitylene (10.0 g, 83.3 mmol) in dry CCl_4 (200 cm^3); the mixture was heated to reflux for 3 h. The orange solution was allowed to cool and the resulting white precipitate was removed by filtration. The solution was then concentrated to an orange oil which was purified by column chromatography on alumina, eluting with hexane, yielding the mixture of inseparable isomers 1,3-bis(bromomethyl)-5-methyl-benzene (the desired product) and 1-(dibromomethyl)-3,5-dimethyl-benzene (undesired by-product) as a white solid (R_f 0.55, 10% DCM–hexane). This mixture of isomers (6.4 g, 23.0 mmol), 3-(2-pyridyl)pyrazole (7.5 g, 51.7 mmol), aqueous NaOH (10 M, 25 cm^3), toluene (100 cm^3) and Bu_4NOH (40% aqueous solution, 3 drops) was stirred vigorously at 60° for 3 h. The mixture was diluted with H_2O (100 cm^3) and the organic layer separated, dried over MgSO_4 and concentrated before purification by alumina column (CH_2Cl_2 : *thf*, 19 : 1) to give L^{mTol} (R_f 0.26) as a white powder (Yield: 5.24 g, 25%). ^1H NMR (250 MHz, CDCl_3): δ 8.62 (2H, ddd, *J* 4.9, 1.8, 0.9; pyridyl H⁶), 7.92 (2H, dt, *J* 7.9, 0.9; pyridyl H³), 7.70 (2H, td, *J* 7.9, 1.8; pyridyl H⁴), 7.39 (2H, d, *J* 2.4; pyrazolyl H⁵), 7.19 (2H, ddd, *J* 7.3, 4.9, 1.2; pyridyl H⁵),

6.97 (2H, s; phenyl H^{4/6}), 6.95 (1H, s; phenyl H²), 6.89 (2H, d, *J* 2.1; pyrazolyl H⁴), 5.32 (4H, s; CH₂), 2.27 (3H, s; CH₃). EI-MS *m/z* 406 (M⁺). Found: C, 73.1; H, 5.4; N, 20.3%. Required for C₂₅H₂₂N₆·(H₂O)_{0.25}: C, 73.1; H, 5.5; N, 20.5%.

Complexes with Ag(I)

Complexes of the ligands with Ag(I) were prepared by combining equimolar quantities of Ag(MeCN)₄BF₄ or Ag(ClO₄) with the appropriate ligand in distilled acetonitrile. Single crystals suitable for X-ray crystallographic and other analyses were grown by slow diffusion of diisopropyl ether into these solutions. Characterisation data for the complexes were as follows:

[Ag(L^{mPh})(BF₄)]_∞. ¹H NMR (250 MHz, CD₃CN): δ 8.19 (2H, ddd, *J* 4.9, 1.5, 0.9; pyridyl H⁶), 7.93 (2H, dd, *J* 7.0, 1.5; pyridyl H⁴), 7.89 (2H, ddd, *J* 7.9, 1.8, 0.9; pyridyl H³), 7.85 (2H, d, *J* 2.4; pyrazolyl H⁵), 7.36 (2H, ddd, *J* 7.0, 5.2, 1.8; pyridyl H⁵), 7.32 (1H, s; phenyl H⁵), 7.09 (1H, s; phenyl H²), 7.08 (2H, s; phenyl H^{4/6}), 6.94 (2H, d, *J* 2.4; pyrazolyl H⁴), 5.17 (4H, s; CH₂). Found: C, 49.3; H, 3.5; N, 14.5%. Required for AgC₂₄H₂₀N₆BF₄: C, 49.1; H, 3.4; N, 14.3%. ESMS: *m/z* 499.1 {Ag(L^{mPh})⁺}, 1087.2 {Ag₂(L^{mPh})₂(BF₄)⁺}, 1675.3 {Ag₆(L^{mPh})₆(BF₄)₄}²⁺, 1968.3 {Ag₇(L^{mPh})₇(BF₄)₅}²⁺, 2261.4 {Ag₈(L^{mPh})₈(BF₄)₆}²⁺, 2555.4 {Ag₉(L^{mPh})₉(BF₄)₇}²⁺, 2848.4 {Ag₁₀(L^{mPh})₁₀(BF₄)₈}²⁺.

[Ag₂(L^{mTol})₂][BF₄]₂. ¹H NMR (250 MHz, CD₃CN): δ 8.30 (2H, ddd, *J* 4.9, 1.8, 0.9; pyridyl H⁶), 7.93 (2H, dd, *J* 6.7, 1.5; pyridyl H⁴), 7.90 (2H, ddd, *J* 7.9, 1.8, 0.9; pyridyl H³), 7.86 (2H, d, *J* 2.4; pyrazolyl H⁵), 7.38 (2H, ddd, *J* 7.0, 4.9, 1.8; pyridyl H⁵), 7.08 (1H, s; phenyl H²), 6.96 (2H, d, *J* 2.4; pyrazolyl H⁴), 6.74 (2H, s; phenyl H^{4/6}), 5.02 (4H, s; CH₂), 1.42 (3H, s; CH₃). Found: C, 49.8; H, 3.5; N, 13.9%. Required for Ag₂(C₂₅H₂₂N₆)₂(BF₄)₂: C, 50.0; H, 3.7; N, 14.0%. ESMS: *m/z* 513.1 {Ag(L^{mTol})⁺}, 1115.2 {Ag₂(L^{mTol})₂(BF₄)₁}⁺, 1717.3 {Ag₆(L^{mTol})₆(BF₄)₄}²⁺, 2016.9 {Ag₇(L^{mTol})₇(BF₄)₅}²⁺, 2317.4 {Ag₈(L^{mTol})₈(BF₄)₆}²⁺, 2618.5 {Ag₉(L^{mTol})₉(BF₄)₇}²⁺, 2918.6 {Ag₁₀(L^{mTol})₁₀(BF₄)₈}²⁺.

[Ag₂(L^{pPh})₂][BF₄]₂. ¹H NMR (250 MHz, CD₃CN): δ 8.38 (2H, d, *J* 5.2; pyridyl H⁶), 7.97–7.86 (4H, m; pyridyl H³ and H⁴), 7.78 (2H, d, *J* 2.4; pyrazolyl H⁵), 7.38 (2H, ddd, *J* 7.0, 4.9, 1.8; pyridyl H⁵), 6.99 (2H, d, *J* 2.4; pyrazolyl H⁴), 6.02 (4H, s; phenyl), 4.85 (4H, s; CH₂). Found: C, 48.2; H, 3.4; N, 14.1%. Required for Ag₂(C₂₄H₂₀N₆)₂(BF₄)₂·(H₂O): C, 48.4; H, 3.6; N, 14.1%. ESMS: *m/z* 500.1 {Ag₂(L^{pPh})₂}²⁺, 1085.2 {Ag₂(L^{pPh})₂(BF₄)⁺}.
[Ag(L^{biph})(BF₄)(MeNO₂)]_∞. ¹H NMR (250 MHz, CD₃CN): δ 8.03 (2H, d, *J* 4.9; pyridyl H⁶), 7.92 (2H, d, *J* 2.4; pyrazolyl H⁵), 7.57 (2H, td, *J* 7.8, 1.8; pyridyl H⁴), 7.69 (2H, d, *J* 7.9; pyridyl H³), 7.26 (2H, ddd, *J* 7.6, 4.9, 1.5; pyridyl H⁵), 7.05–6.90 (6H, m; phenyl), 6.87 (2H, br s; phenyl), 6.75 (2H, d, *J* 2.4; pyrazolyl H⁴), 5.03 (4H, s; CH₂). Found: C, 50.0; H, 4.0; N, 11.6%. Required for Ag(C₃₀H₂₄N₆)(BF₄)·3(H₂O): C, 50.2; H, 4.2; N, 11.7%. ESMS: *m/z* 576.1 {Ag₂(L^{biph})₂}²⁺, 1239.2 {Ag₂(L^{biph})₂(BF₄)⁺}, 1903.4 {Ag₆(L^{biph})₆(BF₄)₄}⁴⁺.

[Ag₄(L^{mes})₃(BF₄)₄]_∞. ¹H NMR (250 MHz, CD₃CN): δ 7.91 (3H, d, *J* 4.9; pyridyl H⁶), 7.85–7.77 (6H, m; pyridyl H³/H⁴), 7.69 (3H, d, *J* 2.4 pyrazolyl), 7.23 (3H, ddd, *J* 7.3, 5.0, 2.3; pyridyl H⁵), 7.79 (3H, d, *J* 2.5; pyrazolyl), 5.44 (6H, s; CH₂), 2.20 (9H, s; methyl). Found: C, 50.3; H, 3.9; N, 14.4%. Required for Ag₄(C₃₆H₃₃N₉)₃(BF₄)₄·2H₂O: C, 50.8; H, 3.9; N,

14.8%. ESMS: *m/z* 700.2 {Ag(L^{mes})⁺}, 1485.4 {Ag₂(L^{mes})₂(BF₄)⁺}, 1680.3 {Ag₃(L^{mes})₃(BF₄)₂}⁺, 2074.4 {Ag₂(L^{mes})₃(BF₄)⁺}, 2271.6 {Ag₃(L^{mes})₃(BF₄)₂}⁺, 2466.6 {Ag₄(L^{mes})₃(BF₄)₃}⁺.

Complexes with Hg(I) and Hg(II)

Complexes with Hg(I) or Hg(II) were prepared by mixing equimolar quantities of ligand and Hg(ClO₄)₂ in nitromethane (for L^{oPh}, L^{pPh} and L^{biph}) or dimethylformamide (for L^{mPh}). Single crystals suitable for X-ray crystallographic and other analyses were grown by slow diffusion of diisopropyl ether into these solutions. Characterisation data for the complexes were as follows:

[Hg(L^{oPh})]₂[ClO₄]₂. ¹H NMR (400 MHz, CD₃NO₂): δ 8.85 (2H, ddd, *J* 5.3, 0.9, 0.6; pyridyl H⁶), 8.41 (2H, td, *J* 7.8, 1.6; pyridyl H⁴), 8.35 (2H, ddd, *J* 7.9, 1.6, 0.9; pyridyl H³), 7.94 (2H, ddd, *J* 7.3, 5.6, 1.8, pyridyl H⁵), 7.87 (2H, d, *J* 2.6; pyrazolyl), 7.69–7.64 (2H, m; phenyl), 7.61–7.56 (2H, m; phenyl), 7.28 (2H, d, *J* 2.4; pyrazolyl), 5.44 (4H, s, CH₂). Found: C, 35.3; H, 2.4; N, 8.7%. Required for Hg(C₂₄H₂₀N₆)(ClO₄)₂·H₂O: C, 35.6; H, 2.7; N, 8.8%. ESMS: *m/z* 297.1 {Hg(C₂₄H₂₀N₆)²⁺}, 493.2 {Hg(C₂₄H₂₀N₆)₂}²⁺, 693.1 {Hg(C₂₄H₂₀N₆)(ClO₄)⁺}, 1085.3 {Hg(C₂₄H₂₀N₆)₂(ClO₄)⁺}, 1484.1 {Hg₂(C₂₄H₂₀N₆)₂(ClO₄)₃}⁺.

[Hg₂(L^{oPh})(MeNO₂)₂][ClO₄]₂. Crystals of this were isolated in small amounts mixed in with crystals of [Hg(L^{oPh})]₂[ClO₄]₂ when the recrystallisation was carried out slowly (weeks). ESMS: *m/z* 693.1 {Hg(C₂₄H₂₀N₆)(ClO₄)⁺}, 1285.2 {Hg₂(C₂₄H₂₀N₆)₂(ClO₄)⁺}.
[Hg₂(L^{mPh})(dmf)₂][ClO₄]₂. ¹H NMR (400 MHz, CD₃NO₂): δ 8.69 (2H, d, *J* 4.4; pyridyl H⁶), 8.28–8.20 (6H, m), 7.89 (1H, s; phenyl H²), 7.81 (2H, pseudo-t, *J* 5.5; pyridyl H⁴ or H⁵), 7.48 (1H, t, *J* 7.9, phenyl H⁵), 7.25–7.21 (4H, m), 5.70 (4H, s, CH₂). Found: C, 31.2; H, 2.6; N, 9.1%. Required for C₃₀H₃₄N₈Cl₂Hg₂O₁₀: C, 31.6; H, 3.0; N, 9.8%. ESMS: *m/z* 397.1 {Hg₂(L^{mPh})₂}²⁺, 592.1 {Hg₂(L^{mPh})₂}²⁺, 893.1 {Hg₂(L^{mPh})(ClO₄)⁺}, 985.3 {Hg(L^{mPh})₂}⁺, 1283.2 {Hg₂(L^{mPh})₂(ClO₄)⁺}, 1885.1 {Hg₄(L^{mPh})₂(ClO₄)₃}⁺.

[Hg₂(L^{pPh})]₂[ClO₄]₂. ESMS *m/z* 397.1 {Hg₂(L^{pPh})₂}²⁺, 593.1 {Hg₂(L^{pPh})₂}²⁺, 893.1 {Hg₂(L^{pPh})(ClO₄)⁺}, 985.3 {Hg(L^{pPh})₂}⁺, 1285.2 {Hg₂(L^{pPh})₂(ClO₄)⁺}, 1377.5 {Hg(L^{pPh})₃}⁺, 1885.1 {Hg₄(L^{pPh})₂(ClO₄)₃}⁺. Found: C, 29.4; H, 2.2; N, 8.7%. Required for C₂₄H₂₀N₆Cl₂Hg₂O₈: C, 29.0; H, 2.0; N, 8.5%. The crystals were not sufficiently soluble to obtain a ¹H NMR spectrum.

[Hg₄(L^{biph})₆][ClO₄]₈·(MeNO₂)₃. ESMS: *m/z* 335.1 {Hg(L^{biph})²⁺}, 569.2 {Hg(L^{biph})₂}²⁺, 769.1 {Hg(L^{biph})(ClO₄)⁺}, 1002.7 {Hg₄(L^{biph})₆(ClO₄)₄}⁴⁺, 1370.3 {Hg₄(L^{biph})₆(ClO₄)₅}³⁺, 2105.4 {Hg₄(L^{biph})₆(ClO₄)₆}²⁺. Found: C, 29.8; H, 2.0; N, 8.8%. Required for C₁₈₀H₁₄₄N₃₆Cl₈Hg₄O₃₂·(0.25dmf): C, 29.4; H, 2.0; N, 8.7%. For ¹H NMR data, see main text.

[Hg₃(L²³²)₂](ClO₄)₆·6MeCN. This was isolated in good yield as the main product from combination of L²³² with Hg(ClO₄)₂ in MeCN. ¹H NMR (270 MHz, CDCl₃): δ 8.56 (2H, d, *J* 5.2; pyridyl H⁶), 8.30–8.15 (5H, m; pyridyl H⁴ all, pyridyl H³ terminal rings), 8.09 (2H, d, *J* 7.3; pyridyl H³ central ring), 8.00 (2H, d, *J* 2.4; pyrazolyl), 7.88 (2H, d, *J* 2.4; pyrazolyl), 7.79 (2H, td, *J* 7.0, 5.7; pyridyl H⁵), 7.22–7.19 (4H, m; pyrazolyl), 5.65 (4H, d, *J* 8.2; phenyl), 5.59 (4H, d, *J* 8.2; phenyl), 5.13 (2H, d, *J* 16.2; CH₂), 4.88 (2H, d, *J* 16.2; CH₂), 4.58 (2H, d, *J* 16.2; CH₂), 3.80 (2H, d, *J* 16.2; CH₂). Found: C, 37.9; H,

2.8; N, 11.3%. Required for $\text{Hg}_3(\text{C}_{43}\text{H}_{35}\text{N}_{11})_2(\text{ClO}_4)_6 \cdot 6\text{H}_2\text{O}$: C, 38.0; H, 3.0; N, 11.3%. ESMS: m/z 422.7 $\{\text{Hg}_3(\text{L}^{232})_2(\text{ClO}_4)\}^{5+}$, 553.1 $\{\text{Hg}_3(\text{L}^{232})_2(\text{ClO}_4)_2\}^{4+}$, 770.5 $\{\text{Hg}_3(\text{L}^{232})_2(\text{ClO}_4)_3\}^{3+}$, 1205.2 $\{\text{Hg}_3(\text{L}^{232})_2(\text{ClO}_4)_4\}^{2+}$.

$[\text{Hg}_3(\text{L}^{232}_{-\text{H}})_2](\text{ClO}_4)_4 \cdot 3\text{MeNO}_2$. This was isolated as the minor component from the above recrystallisation. ESMS: m/z 502.6 $\{\text{Hg}_3(\text{L}^{232}_{-\text{H}})_2\}^{4+}$, 703.5 $\{\text{Hg}_3(\text{L}^{232}_{-\text{H}})_2(\text{ClO}_4)\}^{3+}$, 1105.2 $\{\text{Hg}_3(\text{L}^{232}_{-\text{H}})_2(\text{ClO}_4)_2\}^{2+}$. Found: C, 41.2; H, 3.1; N, 12.6%. Required for $\text{Hg}_3(\text{C}_{43}\text{H}_{34}\text{N}_{11})_2(\text{ClO}_4)_4 \cdot 5(\text{H}_2\text{O})$: C, 41.3; H, 3.2; N, 12.3%.

X-Ray crystallography

A summary of the details of the crystal data, data collection and refinement details is given in Table 14. All structural determinations were carried out using Bruker SMART-1000 or APEX-2 CCD diffractometers equipped with Mo–K α X-radiation at the University of Sheffield, apart from (i) $[\text{Ag}_2(\text{L}^{\text{PPh}})_2][\text{BF}_4]_2$ which was analysed at the University of Bristol on a Bruker PROTEUM CCD diffractometer equipped with Cu–K α radiation from a rotating-anode source, and (ii) $\{[\text{Ag}_4(\text{L}^{\text{mes}})_3](\text{BF}_4)_4\}_\infty$ for which data were collected at the Daresbury Synchrotron Radiation Source (station 9.8) using a Bruker SMART-APEX2 diffractometer and Si(111)-monochromatized synchrotron radiation with a wavelength close to the Zr absorption edge. In all cases, absorption corrections were applied using SADABS,²³ and structure solution and refinement was carried out using SHELXS-97 and SHELXL-97 respectively.²⁴ The structures were solved by direct methods or heavy atom Patterson methods and refined by full-matrix least-squares methods on F^2 . Hydrogen atoms were placed geometrically and refined with a riding model and with U_{iso} constrained to be 1.2 (1.5 for methyl groups) times U_{eq} of the carrier atom. All non-hydrogen atoms were refined anisotropically except where stated otherwise below.

CCDC reference numbers 609491–609503. For crystallographic data in CIF or other electronic format see DOI: 10.1039/b607541j

For $[\text{Ag}(\text{L}^{\text{MPh}})(\text{BF}_4)(\text{iPr}_2\text{O})_{0.5}]_\infty$ the iPr_2O molecule in the symmetric unit was in a general position but refined satisfactorily with a site occupancy of 0.5 for all atoms; geometric restraints were used to keep the geometry of this molecule reasonable. The structural determinations of $[\text{Ag}_2(\text{L}^{\text{MToI}})_2](\text{ClO}_4)_2$ and $[\text{Ag}_2(\text{L}^{\text{PPh}})_2](\text{BF}_4)_2$ were straightforward.

Crystals of $[\text{Ag}(\text{L}^{\text{biph}})(\text{BF}_4)(\text{MeNO}_2)]_\infty$, although of a reasonable size, scattered very weakly and only data with $2\theta \leq 45^\circ$ were used in the final refinement. The asymmetric unit contains two formula units, *i.e.* two independent Ag(I) ions and two ligand molecules. Both of the $[\text{BF}_4]^-$ anions in the asymmetric unit exhibited disorder; in one case the B atom was fixed but the F atoms were disordered over two orientations with site occupancies of 50% in each; in the other case the entire anion was disordered over two sites with site occupancies of 50% in each. All B and F atoms were refined with isotropic displacement parameters. Extensive use of geometric restraints (*e.g.* all aromatic rings flat; equivalent atom–atom separations in different aromatic rings restrained to be similar), and restraints on the displacement parameters, was required to keep the refinement stable. The esd's on the metric parameters are accordingly high for this structure, although the gross geometry is perfectly clear.

In crystals of $[\text{Ag}(\text{L}^{\text{biph}})(\text{BF}_4)(\text{iPr}_2\text{O})_{0.5}(\text{dmf})_{0.25}]_\infty$ the two independent anions in the asymmetric unit were each disordered

over two sites with occupation factors of 0.33/0.67 for the anion containing B(1), and 0.44/0.56 for the anion containing B(2); these B and F atoms were refined with isotropic displacement parameters. The dmf molecule is disordered over a twofold axis which runs through the central C–N bond, such that half of the molecule lies in the asymmetric unit; these atoms were also refined isotropically.

Crystals of $\{[\text{Ag}_4(\text{L}^{\text{mes}})_3](\text{BF}_4)_4\}_\infty$ were tiny (that used had dimensions of $0.20 \times 0.04 \times 0.002 \text{ mm}^3$) and required synchrotron radiation to give a final $R1$ value of 14.1%. Within the limits of the data the gross structure of the coordination network (the asymmetric unit contains four metal cations and three ligands) is well defined although, as with the previous case, the esd's on the metric parameters are high and bond distances and angles should not be over-interpreted. It was possible to locate only 1.5 of the expected four $[\text{BF}_4]^-$ anions; two were located in general positions but one was refined with a site occupancy of 50% to keep the thermal displacement parameters reasonable. Similarity restraints were used extensively during the refinement (*e.g.* all six-membered rings were restrained to be similar, as were all five-membered rings; all B–F distances were likewise restrained to be similar).

The structural determinations of $[\text{Hg}(\text{L}^{\text{Oph}})](\text{ClO}_4)_2$ and $[\text{Hg}_2(\text{L}^{\text{MPh}})(\text{dmf})_2](\text{ClO}_4)_2$ were straightforward and presented no problems. Crystals of $[\text{Hg}_2(\text{L}^{\text{Oph}})(\text{MeNO}_2)_2](\text{ClO}_4)_2$ scattered only very weakly. One of the perchlorate anions was disordered over two sites and refined with a 50% site occupancy in each; the atoms involved were refined with isotropic displacement parameters. In addition, atoms C(12) and C(52) of the ligand needed to be refined isotropically to prevent them from becoming 'non-positive-definite' during refinement. In $[\text{Hg}_2(\text{L}^{\text{PPh}})](\text{ClO}_4)_2$ one of the four independent perchlorate ions was also disordered, with the central atom [Cl(2)] fixed but the set of four oxygen atoms occupying one of three sites with occupancies of 37, 35 and 28%. These oxygen atoms were refined with isotropic displacement parameters, restraints were applied to the Cl–O and O...O separations, and to the displacement parameters of the oxygen atoms.

Crystals of $[\text{Hg}_4(\text{L}^{\text{biph}})_6 \subset \text{ClO}_4][\text{ClO}_4]_7 \cdot (\text{MeNO}_2)_3$ scattered weakly and, like other structural determinations of large cages, the refinement presented several problems. In the cage superstructure only the Hg atoms could be refined with anisotropic displacement parameters, and extensive use of geometric restraints helped to ensure that all aromatic rings were flat with all pyridyl rings having similar geometries to one another and all pyrazolyl rings having similar geometries to one another. The eight perchlorate anions were located in 17 sites with site occupancies of 100% (two cases, refined anisotropically), 50% (nine cases, refined isotropically) or 25% (six cases, refined isotropically); for the sites with occupancies of 50 or 25% extensive use was made of geometric restraints to keep the structures of the anions reasonable. The three nitromethane solvent molecules were located at five sites (one with 100% occupancy and four with 50% occupancy); all were refined with isotropic displacement parameters and were restrained to have similar geometries. Given the extensive disorder and weak scattering the $R1$ value of 11.8% is very reasonable.

The structural determination of $[\text{Hg}_3(\text{L}^{232})_2](\text{ClO}_4)_6 \cdot 6\text{MeCN}$ presented no problems. For $[\text{Hg}_3(\text{L}^{232}_{-\text{H}})_2](\text{ClO}_4)_4 \cdot 3\text{MeNO}_2$ one of the perchlorate anions was disordered over two sites (50% site occupancy in each); the Cl atoms involved could be refined with

anisotropic displacement parameters, but the oxygen atoms all needed to be refined with fixed isotropic displacement parameters. Two of the three lattice solvent molecules were well-behaved and refined anisotropically; the third required geometric restraints and was refined with fixed isotropic displacement parameters to keep the refinement stable.

Acknowledgements

We thank the EPSRC and University of Sheffield for financial support. We also thank EPSRC for funding of the UK National Crystallography Service, and CCLRC (UK) for access to synchrotron facilities.

References

- (a) D. L. Caulder and K. N. Raymond, *Acc. Chem. Res.*, 1999, **32**, 975; (b) G. F. Swieggers and T. J. Malefetse, *Chem.–Eur. J.*, 2001, **7**, 3637; (c) B. J. Holliday and C. A. Mirkin, *Angew. Chem., Int. Ed.*, 2001, **40**, 2022; (d) D. Philp and J. F. Stoddart, *Angew. Chem., Int. Ed. Engl.*, 1996, **35**, 1155; (e) S. Leininger, B. Olenyuk and P. J. Stang, *Chem. Rev.*, 2000, **100**, 853; (f) S. R. Seidel and P. J. Stang, *Acc. Chem. Res.*, 2002, **35**, 972; (g) L. K. Thompson, *Coord. Chem. Rev.*, 2002, **233**, 193; (h) M. Fujita, M. Tominaga, A. Hori and B. Therrien, *Acc. Chem. Res.*, 2005, **38**, 369; (i) D. Fiedler, D. H. Leung, R. G. Bergman and K. N. Raymond, *Acc. Chem. Res.*, 2005, **38**, 349.
- J.-M. Lehn, A. Rigault, J. Siegel, J. Harrowfield, B. Chevrier and D. Moras, *Proc. Natl. Acad. Sci. U. S. A.*, 1987, **84**, 2565.
- M.-T. Youinou, N. Rahmouni, J. Fischer and J. A. Osborn, *Angew. Chem., Int. Ed. Engl.*, 1992, **31**, 733.
- T. Beissel, R. E. Powers and K. N. Raymond, *Angew. Chem., Int. Ed. Engl.*, 1996, **35**, 1084.
- (a) J. S. Fleming, K. L. V. Mann, C.-A. Carraz, E. Psillakis, J. C. Jeffery, J. A. McCleverty and M. D. Ward, *Angew. Chem., Int. Ed.*, 1998, **37**, 1279; (b) R. L. Paul, Z. R. Bell, J. C. Jeffery, J. A. McCleverty and M. D. Ward, *Proc. Natl. Acad. Sci. U. S. A.*, 2002, **99**, 4883; (c) Z. R. Bell, J. C. Jeffery, J. A. McCleverty and M. D. Ward, *Angew. Chem., Int. Ed.*, 2002, **41**, 2515; (d) Z. R. Bell, L. P. Harding and M. D. Ward, *Chem. Commun.*, 2003, 2432; (e) R. L. Paul, S. P. Argent, J. C. Jeffery, L. P. Harding, J. M. Lynam and M. D. Ward, *Dalton Trans.*, 2004, 3453; (f) S. P. Argent, T. Riis-Johannessen, J. C. Jeffery, L. P. Harding and M. D. Ward, *Chem. Commun.*, 2005, 4647; (g) S. P. Argent, H. Adams, T. Riis-Johannessen, J. C. Jeffery, L. P. Harding and M. D. Ward, *J. Am. Chem. Soc.*, 2006, **128**, 72; (h) S. P. Argent, H. Adams, L. P. Harding and M. D. Ward, *Dalton Trans.*, 2006, 542; (i) S. P. Argent, H. Adams, T. Riis-Johannessen, J. C. Jeffery, L. P. Harding, O. Mamula and M. D. Ward, *Inorg. Chem.*, 2006, in press; (j) S. P. Argent, H. Adams, L. P. Harding, T. Riis-Johannessen, J. C. Jeffery and M. D. Ward, *New J. Chem.*, 2005, **29**, 904.
- Self-assembly mediated by Ag...Ag interactions: (a) J. Moussa, K. Boubekeur and H. Amouri, *Eur. J. Inorg. Chem.*, 2005, 3808; (b) Q. L. Chu, D. C. Swenson and L. R. MacGillivray, *Angew. Chem., Int. Ed.*, 2005, **44**, 3569; (c) L. Dobrzanska, H. G. Raubenheimer and L. J. Barbour, *Chem. Commun.*, 2005, 5050; (d) A. A. Mohamed, L. M. Perez and J. P. Fackler, *Inorg. Chim. Acta*, 2005, **258**, 1657; (e) H. P. Zhang, Y. B. Wang, X. C. Huang, Y. Y. Lin and X. M. Chen, *Chem.–Eur. J.*, 2005, **11**, 552.
- Hg...Hg interactions: C. E. Holloway and M. Melic, *J. Organomet. Chem.*, 1995, **495**, 1; A. J. Faville, W. Henderson, T. J. Mathieson and B. K. Nicholson, *J. Organomet. Chem.*, 1999, **580**, 363; X. Wang and L. Andrews, *Inorg. Chem.*, 2004, **43**, 7146; W.-Y. Wong, L. Liu and J.-X. Shi, *Angew. Chem., Int. Ed.*, 2003, **42**, 4064; W.-Y. Wong, K.-H. Choi, G.-L. Lu and Z. Lin, *Organometallics*, 2002, **21**, 4475; K. R. Flower, V. J. Howard, S. Naguthney, R. G. Pritchard, J. E. Warren and A. T. McGown, *Inorg. Chem.*, 2002, **41**, 1907; W.-Y. Wong, G.-L. Liu, L. Li, J.-X. Shi and Z. Lin, *Eur. J. Inorg. Chem.*, 2004, 2066.
- L. Han and M. Hong, *Inorg. Chem. Commun.*, 2005, **8**, 406.
- H. Nierengarten, J. Rojo, E. Leize, J.-M. Lehn and A. Van Dorsselaer, *Eur. J. Inorg. Chem.*, 2002, 573.
- (a) S. Tavecchi, T. A. Miller, R. L. Paul, J. C. Jeffery and M. D. Ward, *Polyhedron*, 2003, **22**, 507; (b) B. Wu, W.-J. Zhang, S.-Y. Yu and X.-T. Wu, *J. Chem. Soc., Dalton Trans.*, 1997, 1795; (c) S. P. Anthony and T. P. Radhakrishnan, *Chem. Commun.*, 2004, 1058; (d) R. H. Wang, M. C. Hong, W. P. Su, Y. C. Liang, R. Cao, Y. J. Zhao and J. B. Weng, *Inorg. Chim. Acta*, 2001, **323**, 139; (e) R. H. Wang, L. J. Xu, X. S. Li, Y. M. Li, Q. Shi, Z. Y. Zhou, M. C. Hong and A. S. C. Chan, *Eur. J. Inorg. Chem.*, 2004, 1595; (f) K. Nomiyama, S. Takahashi, R. Satomi, S. Nemoto, T. Takayama and M. Oda, *Inorg. Chem.*, 2000, **39**, 3301; (g) A. Erxleben, *Inorg. Chem.*, 2001, **40**, 2928; (h) E. Psillakis, J. C. Jeffery, J. A. McCleverty and M. D. Ward, *J. Chem. Soc., Dalton Trans.*, 1997, 1645; (i) P. L. Caradoc Davies, L. R. Hanton and W. Henderson, *J. Chem. Soc., Dalton Trans.*, 2001, 2749; (j) T. K. Ronson, H. Adams and M. D. Ward, *Eur. J. Inorg. Chem.*, 2005, 4533; (k) C. M. Fitchett and P. J. Steel, *Aust. J. Chem.*, 2006, **59**, 19.
- (a) X. Sun, D. W. Johnson, D. L. Caulder, K. N. Raymond and E. H. Wong, *J. Am. Chem. Soc.*, 2001, **123**, 2752; (b) A. M. Garcia-Deibe, J. S. Metalobos, M. Fondo, M. Vazquez and M. R. Bermejo, *Inorg. Chim. Acta*, 2004, **357**, 2561; (c) X. Sun, D. W. Johnson, K. N. Raymond and E. H. Wong, *Inorg. Chem.*, 2001, **40**, 4504; (d) Y. P. Cai, C. Y. Su, C. L. Chen, Y. M. Li, B. S. Kang, A. S. C. Chan and W. Kaim, *Inorg. Chem.*, 2003, **42**, 163; (e) W. Schuh, H. Kopacka, K. Wurst and P. Peringer, *Eur. J. Inorg. Chem.*, 2002, 2202; (f) M. Albrecht, I. Janser, H. Houjou and R. Frohlich, *Chem.–Eur. J.*, 2004, **10**, 2839; (g) M. Albrecht, *Chem.–Eur. J.*, 1997, **3**, 1466.
- (a) A. J. Amoroso, J. C. Jeffery, P. L. Jones, J. A. McCleverty, E. Psillakis and M. D. Ward, *J. Chem. Soc., Chem. Commun.*, 1995, 1475; (b) S. L. James, E. Lozano and M. Nieuwenhuyzen, *Chem. Commun.*, 2000, 617; (c) D. J. Bray, L. L. Liao, B. Antonioli, K. Gloe, L. F. Lindoy, J. C. McMurtrie, G. Wei and X. Y. Zhang, *Dalton Trans.*, 2005, 2082; (d) H.-K. Liu, W.-Y. Sun, D.-J. Ma, K.-B. Yu and W.-X. Tang, *Chem. Commun.*, 2000, 591; (e) S. Hiraoka, Y. Kubota and M. Fujita, *Chem. Commun.*, 2000, 1509; (f) Y. Bretonnière, M. Mazzanti, R. Wietzke and J. Pécaut, *Chem. Commun.*, 2000, 1543; (g) E. Lindner, M. Khanfar and M. Steimann, *Eur. J. Inorg. Chem.*, 2001, 2411; (h) W.-Y. Sun, J. Fan, T. Okamura, J. Xie, K.-B. Yu and N. Ueyama, *Chem.–Eur. J.*, 2001, **40**, 2557; (i) A. Ikeda, H. Udzu, Z. Zhong, S. Shinkai, S. Sakamoto and K. Yamaguchi, *J. Am. Chem. Soc.*, 2001, **123**, 3872.
- (a) C.-Y. Su, B.-S. Kang, C.-X. Du, Q.-C. Yang and T. C. W. Mak, *Inorg. Chem.*, 2000, **39**, 4843; (b) P. Miller, M. Nieuwenhuyzen, J. P. H. Charmant and S. L. James, *CrystEngComm*, 2004, **6**, 408.
- (a) C. J. Baylies, L. P. Harding, J. C. Jeffery, T. Riis-Johannessen and C. R. Rice, *Angew. Chem., Int. Ed.*, 2004, **43**, 4515; (b) D. Grdenic, B. Kamenar and A. Hergold-Brundic, *Croat. Chim. Acta*, 1979, **52**, 339; (c) N. Masciocchi, G. A. Arduozzoia, A. Maspero, G. La Monica and A. Sironi, *Inorg. Chem.*, 1999, **38**, 3657.
- (a) J. C. Dewan, D. L. Kepert and A. H. White, *J. Chem. Soc., Dalton Trans.*, 1975, 490; (b) D. Taylor, *Aust. J. Chem.*, 1977, **30**, 2647; (c) K. Brodersen and H.-U. Hummel, in *Comprehensive Coordination Chemistry*, ed. G. Wilkinson, R. D. Gillard and J. A. McCleverty, Pergamon, Oxford, 1st edn, 1987, vol. 5, p. 1047.
- (a) D. Bravo-Zhivotovskii, M. Yuzefovich, M. Bendikov, K. Klinkhammer and Y. Apeloig, *Angew. Chem., Int. Ed.*, 1999, **39**, 1100; (b) W. Frank and B. Dincher, *Z. Naturforsch.*, 1987, **42b**, 828; (c) R. Malleier, H. Kopacka, W. Schuh, K. Wurst and P. Peringer, *Chem. Commun.*, 2001, 51.
- M. L. McKee and M. Swart, *Inorg. Chem.*, 2005, **44**, 6975.
- (a) G. B. Deacon, C. L. Raston, D. Tunaley and A. H. White, *Aust. J. Chem.*, 1979, **32**, 2195; (b) D. C. Apperley, W. Clegg, S. Coles, J. L. Coyle, N. Martin, B. Maubert, V. McKee and J. Nelson, *J. Chem. Soc., Dalton Trans.*, 1999, 229.
- (a) B. Soro, S. Stoccoro, G. Minghetti, A. Zucca, M. A. Cinellu, S. Gladioli, M. Manassero and M. Sansoni, *Organometallics*, 2005, **24**, 53; (b) R. V. Parish, J. P. Wright and R. G. Pritchard, *J. Organomet. Chem.*, 2000, **596**, 165; (c) Y. J. Wu, S. Q. Huo, J. F. Gong, X. L. Cui, L. Ding, K. L. Ding, C. X. Du, Y. H. Liu and M. P. Song, *J. Organomet. Chem.*, 2001, **637**, 27; (d) C. W. Chan, S.-M. Peng and C.-M. Che, *Inorg. Chem.*, 1994, **33**, 3656; (e) E. C. Constable, T. A. Leese and D. A. Tocher, *J. Chem. Soc., Chem. Commun.*, 1989, 570.
- Representative examples of metallo-catenates: (a) A. M. L. Fuller, D. A. Leigh, P. J. Lusby, A. M. Z. Slawin and D. B. Walker, *J. Am. Chem. Soc.*, 2005, **127**, 12612; (b) L. Flamigni, A. M. Talarico, J.-C. Chambron, V. Heitz, M. Linke, N. Fujita and J.-P. Sauvage, *Chem.–Eur. J.*, 2004, **10**, 2689; (c) A. Livoreil, J.-P. Sauvage, N. Armaroli, V. Balzani, L. Flamigni and B. Ventura, *J. Am. Chem. Soc.*, 1997, **119**, 12114; (d) D. J. Cardenas and J.-P. Sauvage, *Inorg. Chem.*, 1997, **36**, 2777; C. O. Dietrich-Buchecker, J. Guilhem, A. K. Khemiss, J.-P.

- Kintzinger, C. Pascard and J.-P. Sauvage, *Angew. Chem., Int. Ed. Engl.*, 1987, **26**, 661; (e) A. Hori, K. Yamashita and M. Fujita, *Angew. Chem., Int. Ed.*, 2004, **43**, 5016; (f) A. Hori, K. Yamashita, T. Kusukawa, A. Akasaka, K. Biradha and M. Fujita, *Chem. Commun.*, 2004, 1798; (g) C. Dietrich-Buchecker, B. Colasson, M. Fujita, A. Hori, N. Geum, S. Sakamoto, K. Yamaguchi and J.-P. Sauvage, *J. Am. Chem. Soc.*, 2003, **125**, 5717; (h) M. Fujita, *Acc. Chem. Res.*, 1999, **32**, 53; (i) J.-P. Collin, V. Heitz and J.-P. Sauvage, *Top. Curr. Chem.*, 2005, **262**, 29.
- 21 C. O. Dietrich-Buchecker, J.-P. Sauvage and J. P. Kintzinger, *Tetrahedron Lett.*, 1983, **24**, 5095.
- 22 A. J. Blake, C. O. Dietrich-Buchecker, T. I. Hyde, J.-P. Sauvage and M. Schröder, *J. Chem. Soc., Chem. Commun.*, 1989, 1663.
- 23 G. M. Sheldrick, *SADABS version 2.10*, University of Göttingen, 2003.
- 24 G. M. Sheldrick, *SHELXS-97 and SHELXL-97*, University of Göttingen, 1997.